Review

Advances in Biosensors for Early and Rare Disease Detection: A Fabrication Perspective

Dipti Rupwate * and Gowri Balachander

Posted Date: 14 March 2025

doi: 10.20944/preprints202503.0996.v1

Keywords: biosensor; fabrication; materials; nanoparticles; biomarkers; rare disease; early detection; aptamer; enzyme biosensor

Review

Advances in Biosensors for Early and Rare Disease Detection: A Fabrication Perspective

Dipti Ulhas Rupwate * and Gowri Manohari Balachander

School of Biomedical Engineering, Indian Institute of Technology (BHU) Varanasi, Varanasi, 221005, Uttar Pradesh, India

* Correspondence: diptiulhas.rupwate.bme20@itbhu.ac.in or diptirupwate13@gmail.com

Abstract: The need for early diagnosis of diseases, especially severe and rare diseases, has increased the demand for developing better biosensors for diagnosis. These tools can diagnose diseases at their early stage and sometimes even before the onset of symptoms. This review is focused on the analysis of the methods of biosensor creation and their application for early disease diagnosis. This review includes various categories of biosensors, including nanomaterials, aptamers, and peptides. The focus is on developing these sensors and employing the right materials. Different fabrication techniques are presented, including thin-film deposition, lithography, printing, and microfluidics, due to their merits and disadvantages. This review also examines the effectiveness of these biosensors in clinical practice and various laboratory tests. We also focus on enhancing performance and sensitivity when nanomaterials and nanotechnology are employed. Additionally, we discuss scalability, reproducibility, and suggest ways to overcome these issues. We also describe current and emerging developments in advanced biosensors, including point-of-care and biosensor fusion systems. This review will be helpful for scholars, practitioners, and decision-makers because it concentrates on biosensor design and implementation technology.

Keywords: biosensor; fabrication; materials; nanoparticles; biomarkers; rare disease; early detection; aptamer; enzyme biosensor

1. Introduction

Biosensors are used in the early detection of diseases and provide fast and reliable results for the patient's condition. These tools are intended to identify particular natural markers or analytes related to numerous diseases with the aim of early intervention and commencement of treatment. Recognizing such hints in the early stages of the disease greatly increases the chances of successful treatment and slows the progression of the illness. This is because it leads to enhanced results and better patient general health. The benefits of biosensors are high sensitivity, specificity, and the ability to identify biomarkers in complex biological samples. These qualities are essential for quickly identifying diseases [1].

Mesothelioma is a type of cancer that mainly affects the pleura, which is the protective membrane of the lungs. Asbestos is most often associated with it, and the disease may develop several years after contact with the material [2]. Hepatoblastoma is a very infrequent liver tumor that occurs mainly in children younger than three years of age. It is often associated with genetic disorders and preterm birth; however, the cause of this condition has still not been established. Additionally, cystic hydatid disease, caused by the larval stage of Echinococcus granulosus, forms cysts in the liver and lungs when contaminated materials are consumed [3]. Regarding genetic diseases, cystic fibrosis stems from mutations in the CFTR gene. It leads to the formation of thick secretions in the respiratory and digestive tracts of the body [4]. However, maturity-onset diabetes tends to develop in families and is sometimes identified before age 25 [5]. Finally, pneumonia is a type of infection that affects the air sacs in the lungs. It is caused by bacteria, viruses, or fungi and is particularly dangerous for children, elderly individuals, and immunocompromised individuals [6]. Early identification and

 doi:10.20944/preprints202503.0996.v1

management of these conditions are essential to avoid adverse effects on patient health and improve patient prognosis.

Caring for rare diseases can be challenging since they are not very common, and their manifestations are not always readily noticeable. The identification and management of the disease can be rather complicated. Screening and treating diseases such as mesothelioma, hepatoblastoma, cystic echinococcosis, cystic fibrosis, MODY, and pneumonia are crucial because they reduce the severity of the disease [3–8]. Biosensors present a potential solution in this case because they can effectively identify markers of these diseases. For instance, early diagnosis is essential in mesothelioma since the disease is frequently diagnosed at the final stage, resulting in a poor outcome [7]. Biosensors can be used as specific biomarkers of mesothelioma, enabling early diagnosis of the disease and timely treatment.

Similarly, biosensors are also used to monitor cystic fibrosis development and MODY management for better treatment options. Biosensors are devices widely used in the healthcare industry for quick and efficient diagnosis. This facilitates fast and effective intervention, positively impacting patients' conditions afflicted with rare diseases [9].

There are various types of biosensors, and each technology is more suitable for the detection of biological species. Enzyme-based biosensors are highly specific because enzymes and substrates have a specific relationship [10]. On the other hand, biosensors employ nanomaterials to display high sensitivity due to the increased surface area-to-volume ratio and distinctive electrical characteristics [11]. Additionally, optical biosensors are suitable for real-time noninvasive detection and are, therefore, ideal for in vivo use [12].

The current biosensor fabrication methods provide different benefits regarding biosensor characteristics, such as performance, adaptability, and reproducibility. Micropatterning methods enable control over the shape and size of the sensor, which increases the sensitivity and accuracy of the sensors. This approach provides scalability and reproducibility, which are relevant to mass production [13]. Complex sensor designs can be easily and inexpensively produced using 3D printing. In this way, the method is highly suitable for rapidly developing individualized sensors for specific applications [14]. Lithographic techniques help deliver high-quality and detailed sensor components, thus allowing the formation of complex and very tiny sensor structures. This method is beneficial in applications where detection is critical and needs to be very precise [15]. Some of the measures used to fix the recognition elements on the sensor's surface are crucial in determining its stability and sensitivity. These techniques help in the modification of the surface of sensors with different biomolecules, and thus, the identification of different analytes can be performed with high accuracy.

Disease detection and monitoring is one of the most complicated issues that scientists and medical experts face; however, various biosensors can be used to solve this problem. This can result in enhanced patient care and, therefore, better results.

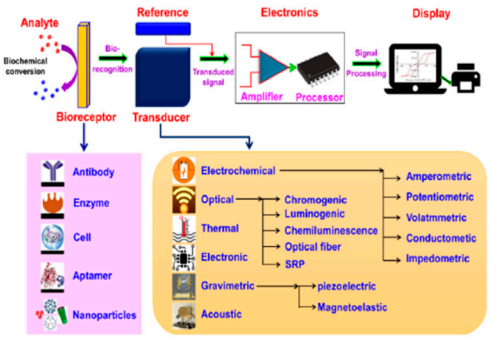

Figure 1. A Schematic of a Biosensor's Design. It also shows common types of bioreceptors and transducers used in biosensors [16].

 doi:10.20944/preprints202503.0996.v1

2. Biosensor Overview

2.1. Components Used in Biosensors

Biosensors can be divided into biological recognition elements, transducers, and signal processing units. The following sections assist in categorizing biosensors according to their characteristics and uses.

2.1.1. Biological Recognition Elements

Biological recognition elements provide the selectivity of the interactions with the analytes. It reacts with a target substance, `analyte,' and creates a discernible biological process. The selectivity and accuracy of the biosensor are directly related to the quality of this particular component. The understanding of poor recognition elements is that they result in false positives and false negatives.

There are various types of biosensors, each with unique features. There are various types of biosensors, each with unique features:

1. Enzyme Biosensors:

Enzyme biosensors have developed over time. First-generation biosensors use natural electron acceptors such as oxygen; however, they suffer from interference. Second-generation biosensors employ synthetic electron acceptors, such as ferrocene, to minimize interference and enhance stability. Third-generation biosensors do not use mediators, which improve their selectivity and stability through direct electron transfer between the enzyme and the electrode. New and improved nanoparticles and immobilization methods have enhanced the sensitivity and reliability of enzyme biosensors [17,18].

2. Antibody Biosensors:

Antibody-type biosensors identify specific substances by using antibodies. It is applied in medical diagnostics, environmental testing, monitoring, and food safety. These biosensors function by immobilizing antibodies on their surface. When they bind target antigens, they generate a signal that can be easily detected. The signal that is generated can be optical, electrochemical, or gravimetric.

Additionally, integrating antibody biosensors with other systems, such as microfluidics and wireless communication, has made it possible to develop portable diagnostic devices. For instance, fiber optic-based antibody biosensors are very sensitive and specific. It also enables the sensing to be performed at a distance and the analysis to be conducted in real-time. This makes them applicable in personal medicine and environmental screening on a massive scale [16,19].

3. Aptamer biosensors:

Due to their high specificity and binding affinity, aptamer-based biosensors, commonly known as aptasensors, are being rapidly developed. Aptamers are short strands of DNA, RNA, or peptides, and biosensors employ them in their detection pattern. This ensures they engage firmly and specifically with molecules, including proteins, cells, and other small molecules.

New studies have revealed the following advancements. Thus, fluorescent aptasensors with mesoporous silica nanoparticles can detect aflatoxin B1 with higher sensitivity and specificity than other methods. This is important in analyzing food products and environmental samples [20]. The significant advantage of using aptamers in point-of-care diagnostics over traditional antibodies is that aptamers can be chemically synthesized. This makes it possible to identify disease biomarkers in a fast and efficient manner [21]. Similar to neurological and cardiovascular diseases, aptamer-based sensors are used to identify neurotransmitters at significantly lower levels to improve the diagnosis and control of diseases [22].

Additionally, aptamer biosensors are efficient at detecting bacterial pathogens. These methods detect bacterial cells and toxins with high specificity and high affinity. It is helpful in minimizing the spread of diseases and controlling outbreaks of infections [23]. All these advancements depict the versatility of aptamer-based biosensors and their potential in different applications.

4. Whole-Cell Biosensors:

 doi:10.20944/preprints202503.0996.v1

Whole-cell biosensors are based on living cells and synthetic biology for enhanced detection. Some of the genetic components included transcription factors and riboswitches. Biosensors are adaptive systems that use gene circuits to identify target substances in the environment. They are also inexpensive to produce, and with the help of biotechnology, they can be easily produced because cells can duplicate themselves. Current developments have made them more flexible and convenient for numerous applications, including food safety, environmental analysis, and wearable health monitoring [24–26].

5. Nanoparticle biosensors:

Nanoparticle biosensors are changing biosensing because they are more sensitive, specific, and versatile. Gold nanoparticle biosensors can quickly detect biomarkers such as retinol-binding protein 4 (RBP4), yielding results in just 5 minutes. This makes them perfect candidates for point-of-care testing [27]. Magnetic nanoparticle biosensors identify cancer biomarkers such as microRNAs (miRNAs) in complex samples. They are biocompatible and easy to modify, which increases their sensitivity and specificity [28]. New nanometer-scale biosensors can also detect a wide range of biomolecules using different recognition elements, such as antibodies and nucleic acids [29].

2.1.2. Transducer

A transducer is a crucial part of biosensors. It changes biological reactions into measurable signals. This allows the biosensor to give a precise result. Transducers are the basis for different types of biosensors. These include electrochemical, electronic, thermal, optical, and mass-based (gravimetric) sensors.

1. Electrochemical Biosensors:

Electrochemical biosensors change biological information into electrical signals. These sensors are essential in healthcare, food safety, and environmental monitoring. They are sensitive, selective, and portable. There are three types: amperometric, potentiometric, and impedimetric. Each type uses different methods to detect substances. Recent advances include the use of nanomaterials such as graphene and carbon nanotubes to improve performance. Machine learning has also been used to better understand sensor data, increasing accuracy. However, there are challenges, such as signal interference and effective immobilization. Future research should focus on creating more reliable designs that resist interference. It also aims to make these sensors easier to use [30,31].

2. Optical Biosensors:

Many advanced optical biosensors use surface plasmon resonance (SPR) and localized surface plasmon resonance (LSPR) technologies. These methods are highly sensitive and can detect objects in real-time.

SPR biosensors work by measuring changes in the refractive index at the sensor surface. Recent improvements have made them more sensitive by adding new nanomaterials and better designs, such as windmill-shaped multichannel SPR sensors that can detect multiple things simultaneously [19,32].

Fiber optic SPR biosensors are helpful for remote and portable applications. It has shown better accuracy in medical and environmental monitoring [19]. LSPR biosensors use metal nanoparticles and are very sensitive. They are being developed for early disease detection and monitoring. Combining them with other platforms makes them even better [32].

3. Gravimetric Biosensors:

Gravimetric biosensors measure mass changes on a sensor surface to detect biological interactions. They are known for their high sensitivity and real-time monitoring.

Recent advancements include MEMS acoustic resonators such as the S1 mode Lamb wave resonator. A 400-nm X-cut lithium niobate film has a resonance frequency of more than 8 GHz and a mass sensitivity of up to 74,000 Hz/(ng/cm^2) [33].

Another innovation involves aluminum nitride (AlN) thin film-based resonators. The resonators have a chemically conjugated surface, enhancing the selectivity and sensitivity for bacterial analysis [34].

 doi:10.20944/preprints202503.0996.v1

A new gravimetric biosensor design addresses acoustic radiation issues in liquid environments. It uses locally resonant photonic crystals to suppress acoustic radiation, improve quality, and reduce frequency noise [35].

4. Thermal Biosensors:

In the recent past, the advancement of thermal biosensors has increased, especially in environmental monitoring and health care. These devices detect temperature fluctuations arising from biochemical processes and are characterized by high sensitivity and early detection. For example, a thermal biosensor with a flow injection analysis system can determine the COD of water samples. The method is stable, has an extensive range, and does not use toxic chemicals [36]. Some changes have been made, including nanoparticles and nanowires, which have enhanced the sensors by increasing the surface area and conductivity [16]. Such enhancements suggest the use of thermal biosensors for constant environmental scanning and nonintrusive real-time health assessment.

5. Electronic Biosensors:

Electronic biosensors use electronic components to identify and quantify biomaterials. They are efficient and precise in their work. It has been established in the recent past that AlGaN/GaN HEMTs are quite effective and selective in detecting proteins and, hence, useful in disease diagnosis. This results from high transconductance and stability, especially in areas of high-power application [37]. Research on GaN/AlN/AlGaN MOSHEMT biosensors presents a new design with a nanogap-embedded cavity. This design enhances the ability to identify biomolecules without labels and is thus recommended for future diagnostic tools [38].

6. Acoustic Biosensor:

Acoustic biosensors employ surface acoustic waves (SAWs) and bulk acoustic waves (BAWs). It is a highly specific device for identifying proteins, DNA, disease markers, and pathogens without real-time labels. Examples of recent advancements include the integration of biosensors with microfluidics to develop lab-on-a-chip systems. This is because it can easily accommodate and analyze small biological samples. New materials that have improved the piezoelectric properties of biosensors include improvements in CRISPR–Cas systems, which have made biosensors more sensitive and specific. Nevertheless, some issues will likely arise, including how to make it more scalable and incorporate it with existing diagnostic tools [39,40].

2.1.3. Signal Processing System

The display and signal-processing unit of biosensors entails the conversion of such biological reactions to electrical signals. The system analyzes and presents the information.

Modern developments in signal processing for biosensors have been made to address some of the issues encountered with conventional methods. One of them is the asymmetric Schottky barrier-generated MoS2/WTe2 field-effect transistor (FET) biosensor. This approach solves problems such as hysteresis and noise by utilizing the "rectified signal" instead of the "absolute value signal." It also enables the detection of the DYRK1A gene associated with Down syndrome with high sensitivity, a detection limit of 10 aM, and a working range of 10 aM to 100 pM [41].

Other scholars also proposed an intelligent GFET biosensor with a signal processing unit for the real-time detection of serotonin with high sensitivity. The algorithm encompasses several data features, increasing the detection effectiveness and dependability, particularly in low-concentration zones where other methods fail [41].

 doi:10.20944/preprints202503.0996.v1

2.2. Method of Surface Modification

Surface modification techniques are necessary because materials need to be enhanced to serve specific purposes. All the methods have their advantages.

1. Chemical Modification:

Chemical modification is helpful in improving the functionality of biosensors. This enhances the bioreceptor's adhesion to the sensor. Another relatively new method is the use of silanes on SiO2 surfaces. It forms a layer with the help of 3-ethoxy dimethylsilyl propylamine (APDMS), which prevents the fouling of the sensor; thus, the sensor can be used for the detection of matrix metalloproteinase 9 (MMP9) [42]. Another way is to modify the surface of gold and CNTs, which results in the formation of strong surface groups that increase the sensitivity and prevent accumulation [43].

2. Coating Deposition:

Different coating deposition methods, such as physical vapor deposition (PVD) and chemical vapor deposition (CVD), enhance the features of biosensors through surface enhancement. Magnetron sputtering and pulsed laser deposition are PVD techniques that provide reasonable control over the film thickness and the element concentration. This method results in hard, thin films with a low friction coefficient, enhances the protection of the sensor surface, and increases the conductivity. CVD techniques are based on chemical reactions of gaseous precursors on the substrate surface, which results in uniform and well-adherent coatings. New developments in CVD techniques, for instance, plasma-assisted CVD (PA-CVD) and in sputtering techniques, such as high-power impulse magnetron sputtering (HIPIMS), have made it possible to produce films with nanostructures and enhanced characteristics. The films are capable of healing themselves and can change their size with the help of stimuli received from biological environments, which decreases the problem of biofouling and increases the sensitivity of the sensors [44,45].

3. Plasma Treatment:

Treatment with plasma, especially oxygen plasma, is one of the most efficient ways to enhance biosensors. For instance, when SPCEs are plasma treated with oxygen, carboxyl groups are introduced on the surface. This enhances the electrochemical performance of these materials and provides more binding sites for the antibodies, resulting in a low detection limit and high sensitivity compared to nonmodified electrodes [46]. The surface roughness and chemical properties can also be altered by plasma treatments. This is observed in the case of reduced graphene oxide surfaces for detecting amyloid-beta peptides in Alzheimer's disease diagnosis [47]. The literature on plasma surface modification techniques indicates that plasma surface modification is the most effective way of producing surfaces with suitable characteristics to enhance biocompatibility and sensor properties [48].

4. Biomolecule Immobilization:

Biomolecule immobilization is an essential step in which biomolecules such as proteins, enzymes, and DNA are anchored on the surface to operate biosensors effectively. Adsorption based on hydrogen bonding, van der Waals forces, and electrostatic interactions is relatively simple, fast, and nondestructive for biomolecules, but it is not as stable as covalent binding. To counter this, covalent bonds create a stable structure with lasting bonds that are chemically stable, do not easily leach out, and stick well to the surface, although more chemical treatment may be required. The encapsulation or entrapment of biomolecules into a matrix or within a membrane can provide better stability and protection than covalent binding, which is affected by complexity. Crosslinking can enhance stability by linking biomolecules and surfaces to avoid leakage. A non-damaging method with limited control is physical entrapment, in which biomolecules are confined within a porous matrix without changing their chemical properties. Additionally, layer-by-layer assembly builds up films by the stepwise adsorption of positively and negatively charged layers, which enables effective control of the immobilization process, albeit at the expense of time [16].

 doi:10.20944/preprints202503.0996.v1

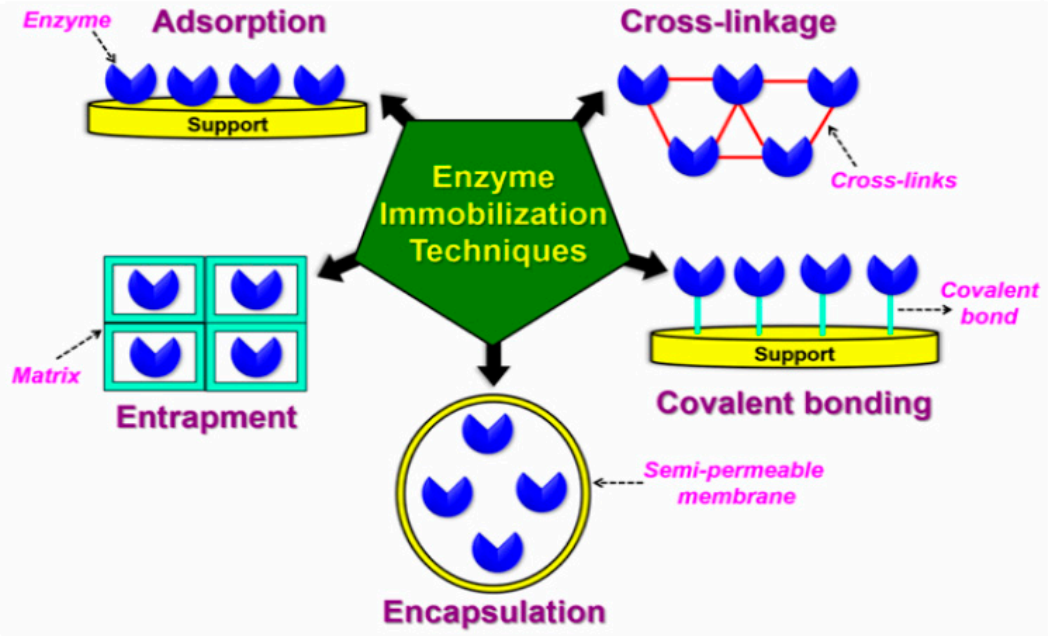

Figure 2. Techniques for Immobilizing Enzymes.It explains the principles and uses of each method, showing how they improve enzyme stability and performance in biosensors [16].

5. Surface Patterning:

This method entails the creation of specific structures or patterns on surfaces. The development of surface patterning for the modification of biosensors has greatly improved with the use of SPR, CLL, and other surface modification approaches to increase the sensitivity and specificity of biosensors. SPR biosensors are based on functionalized gold surfaces and nanomaterial coatings to overcome problems such as nonspecific adsorption and protein fouling, which in turn enhance the sensitivity and real-time detection capability [49]. CLL offers highly accurate nanopatterning of self-assembled monolayers on different metals and can be used to functionalize aptamers on the surface of FET biosensors for the specific and sensitive sensing of biomolecules [50] . Moreover, the surface of the substrate can be modified using UV light treatment for hydrophilicity and the application of nanomaterials to increase its biocompatibility and, in turn, the biosensor's performance [43].

6. Biological Surface Modifications:

This method is used for surface modification in biomedical applications such as cell seeding, tissue engineering, and bioconjugation. Biomaterial biocompatibility is influenced by surface chemistry, roughness, wettability, and charge [51]. For instance, in the case of NiTi, the concentration of ions of Ni released can significantly influence the biocompatibility. The roughness of the surface and its wettability affect cell adhesion [52].

 doi:10.20944/preprints202503.0996.v1

Table 1. Biosensing Techniques and Underlying Principles.This table provides a detailed overview of different biosensing technologies. It explores their surface customization and immobilization methods and the mechanisms that govern their functionality. **Abbreviation**:Biosensing Techniques and Underlying Principles.This table provides a detailed overview of different biosensing technologies. It explores their surface customization and immobilization methods and the mechanisms that govern their functionality. Abbreviations: Self-Assembled Monolayer (SAM), Cyclin-Dependent Kinase 6 (CDK-6), Resonance Energy Transfer (RET), Carbon Screen-Printed Electrode (CSPE), Carboxyl Group (COOH), Gold Nanoparticles (AuNPs), Graphdiyne (GDY), Polyethylene Glycol (PEG), C-Reactive Protein (CRP), Indium Tin Oxide (ITO), Electrochemiluminescence (ECL), Alpha-Fetoprotein (AFP), Fluorescence Resonance Energy Transfer (FRET), 3-Aminopropyl-Triethoxysilane (APTES), Photonic Crystal Slab (PCS), Porous Silicon (PSi), Surface-Enhanced Raman Spectroscopy (SERS), Square Wave Voltammetry (SWV), Metal-Oxide-Semiconductor Field-Effect Transistor (MOSFET), Ion-Sensitive Field-Effect Transistor (ISFET), Potassium Hydroxide (KOH), Silver Nanoparticles (AgNPs), Multi-Walled Carbon Nanotubes (MWCNTs), Gold Nanoparticles (AuNPs), Chitosan-Ionic Liquid (CS-IL), Gold-Lead Nanoparticles (AuPbNPs), Electrochemical Impedance Spectroscopy (EIS), Surface Plasmon Resonance (SPR), Parallel-Parallel Head-to-Head (PPH2H), Electrochemical Surface Impedance (ESI), Charge Transfer Resistance (CTR), Cyclic Voltammetry (CV).

Biosensor	Surface Modification Technique	Immobilization Technique	Working Principle of BS	Reference
Aptamer	Biomolecule Immobilization	Physical Adsorption	Fluorescence proportional to AFP concentration	[53]
Electrochemical	Self-Assembled Monolayer (SAM)	Molecular Imprinting	Measures changes in sensing electrode potential	[54]
Electrochemical	Chemical Modification-Spacer Deposition: Introduction of Cross-Linkers	Cross Linking	Electro kinetics-assisted molecular trapping	[55]
Electrochemical	Chemical Modification (CSPE-COOH-AuNPs)-Amino Coupling Protocol. Chemical Modification (CSPE-AuNPs-SAM)-SAM Formation	CSPE-COOH-AuNPs: Covalent Bonding; CSPE-AuNPs-SAM: Covalent Bonding	Electrochemical signals from anti-CRP and CRP interaction	[56]
Electrochemical	Chemical Modification-Functionalization: GDY (Graphdiyne); Antifouling: with PEG (Polyethylene Glycol).	Physical Entrapment	Signals from biomarker binding to imprinted polymer sites	[1]
Electrochemical	Physical Adsorption- Use of gold (Au) nanowires grown on a Poly Carbonate (PC) substrate	Adsorption	CRP binding to anti-CRP enhances immunosensor signal	[57]
Electrochemical	Chemical Modification-Salinization: Assembly of gold nanoparticles (AuNPs) on the surface of ITO using a hydrolyzed polymer of (3-aminopropyl) trimethoxy silane (APTMS).	Adsorption	Electrochemical luminescence of luminol for C-peptide detection	[58]
Electrochemical	Chemical Modification: Assembly of Nafion solution soaked Ru(II)-organic complex (Ru-PEI-ABEI) onto the electrode surface.	Covalent Bond	C-peptide detection via DNA and dopamine quenching ECL signal	[59]
Electrochemical	Plasma Treatment- Oxygen Plasma Cleaning; Chemical Modification-Salinization with APTES(3-Aminopropyl-triethoxysilane); Functionalization: Glutaraldehyde (Glu) Modification	Covalent Bond	Binding alters surface charge and conductance	[60]
Electrochemical	Chemical Modification-Self-Assembled Monolayer (SAM) Coating Deposition-	Covalent Bond	Reduction current on gold electrode proportional to antibody concentration	[61]

 doi:10.20944/preprints202503.0996.v1

Electrochemical	Physical deposition: Deposition of Gold Nanoparticles Chemical Modification-Functionalization: With Mercaptopropionic Acid (MPA) Chemical Modification – Functionalization: Cysteamine was utilized to create a self-assembled monolayer of alkyl amine groups Electrochemical Activation- Involved cycling the potential from -0.200V to 1.20V for 10 cycles at a rate of 100 mV/s.	Covalent Bond	SWV reduction peak current change with antibody/antigen binding	[62]
Electrochemical	Physical Vapor Deposition (PVD)-Drop casting a suspension of Carbon nanodots (CD)	Adsorption	Target DNA hybridization results in an electrochemical signal	[63]
Electrochemical	Chemical Modification-Functionalization: Modifying Metal-Oxide-Semiconductor Field Effect Transistor (MOSFET) with an electrolyte solution containing ions to create an Ion-Sensitive Field Effect Transistor (ISFET).	-	Source-drain current modulated by gate potential and analyte concentration	[64]
Electrochemical	Chemical Adsorption-Drop-casting solution containing multi-walled carbon nanotubes-graphene-ionic liquid (MWCNTs-Gr-IL). Chemical Deposition-Deposition of 4-amino-N, N, N-trimethylamine (ATA) + 4-amino benzenesulfonate (ABS) by applying electrochemical potential.	Covalent Bond using Electrochemical Immobilization	Bioanalyte-biopreceptor binding reduces response to probe molecules	[65]
Electrochemical	Chemical Adsorption- By graphene-multiwalled carbon nanotubes; Chemical Adsorption-Drop-casting of chitosan-1-ethyl-3-methylimidazolium bis (trifluoromethyl sulfonyl) imide (CS-IL); Coating-Electrodeposition: Deposition of amine-functionalized AuPb NPs	Covalent Bond	Bioreceptor-bio analyte coupling alters impedimetric and amperometric responses	[66]
Electrochemical	-	Covalent Bond	Electroconductivity change with bacteria capture on the electrode	[67]
Electrochemical	Coating-Electrodeposition: Deposition of Pb NPs by cyclic voltammetry (CV) to increase the sensor's surface area	Covalent Bond	Electrochemical impedance spectroscopic (EIS) response change	[68]
Gravimetric	Self-Assembled Monolayer (SAM)	Thiol immobilization	Mass change is inversely proportional to crystal frequency change	[69]
Immunosensor	Chemical Modification-Functionalization: Electroreduction of carboxyphenyl diazonium salt	Covalent Bond	Protein binding changes the electrochemical signal in SWV	[70]
Immunosensor	Chemical Modification-Functionalization: Treating potassium hydroxide (KOH); Chemical Modification- Attaching amine-functionalized silver nanoparticles (AgNp) using chemical linker Glutaraldehyde	Covalent Bond using Glutaraldehyde	Procalcitonin-antibody interaction changes electrode current response	[71]
Nanoparticle	-	Physical Adsorption: Coating the micro-wells with E. granulosus antigen using the sodium carbonate method	Color change by nanoparticle detected by spectrophotometer	[72]

 doi:10.20944/preprints202503.0996.v1

Nucleic Acid	Coating-Electrodeposition: Deposition of Cysteamine/AuNPs on the surface of Au electrodes	-	DNA hybridization changes biosensor electrochemical behavior detected by SWV	[73]
Optical	-	-	Sensor responds to CDK6 activity via fluorescence changes	[74]
Optical	Chemical Modification-Surface Functionalization: Modification using luminol@Au/Ni-Co nanocages.	Covalent Bond	Quenching luminescence for I27L detection via RET	[75]
Optical	Biomolecule Immobilization	Physical Adsorption	Fluorescence Resonance Energy Transfer (FRET)	[12]
Optical	-	-	Refractive index change in PSM measured by near-infrared laser	[76]
Optical	Chemical Modification-Silanization: with a silane compound, 3-aminopropyltriethoxysilane (APTES).	Covalent Bonding-Glutaraldehyde Immobilization	Fluorescence and reflection in porous silicon (PSi)	[77]
Optical	Physical Vapor Deposition (PVD)-Sputtering silver nanoparticles onto the porous silicon substrate.	-	Surface-enhanced Raman Spectroscopy (SERS)	[3]
Optical	Chemical Modification-Functionalization: With Protein A	Covalent Bonding: Antigen was immobilized on a nitrocellulose membrane	Antibody presence causes color change in the complex	[78]
Optical	GQDs exhibit inherent surface characteristics based on their synthesis conditions	-	Fluorescence quenching in graphene quantum dots by chloride ions	[9]
Optical	Chemical Conjugation-Attachment of thiolated DNA probes onto gold nanoparticles (GNPs)	Adsorption	Capillary action binds target DNA to streptavidin, showing a red line	[79]
Optical	Coating-Electron Beam Deposition: On glass surfaces, with titanium (Ti) and gold (Au) coatings. Cleaning Process- By sonication in solvents of high polarity; Chemical Modification: Self Self-assembled monolayer (SAM) formation of thiol.	Covalent Bond	SPR with PPRH probe recognizing DNA sequences	[80]
Optical (FRET)	Coating- Coating the surface with nickel	Coordination Bond: Between the His-tag and nickel coating	FRET signal decreases with fluorescent protein separation	[81]
Optical Microfiber	Chemical Modification-Salinization: with APTES(3-Aminopropyl-triethoxysilane)	Cross Linking	Evanescent wave absorption by GNPs near fiber surface	[82]
Peptide	Surface Patterning-Use of screen printed electrode; Coating-Electrodeposition: of 4-amino-N, N, N-trimethylamine, and 4-amino benzenesulfonate.	Covalent Bond	ESI measures the change in Rct with protein binding	[83]

 doi:10.20944/preprints202503.0996.v1

3. Advancements in Fabrication Methodology

A biosensor has two essential components: biological recognition elements and a transducer. This section discusses the advantages and disadvantages of different fabrication techniques and materials for specific types of biosensors.

3.1. Electrochemical Biosensor

Making electrochemical biosensors involves a few key steps. First, the electrode surface is prepared. Next, it is modified to be biocompatible. Then, biological elements like enzymes or antibodies are added. Techniques like the use of gold nanoparticles improve sensitivity. Screen-printed carbon electrodes help reduce costs and make the devices small and portable.

Molecular imprinting is essential in advancing electrochemical biosensors as it offers selectivity, stability, sensitivity, and compatibility with electrochemical transduction methods. It has many applications, covering various target molecules such as proteins, peptides, small organic molecules, and whole cells. The effectiveness of this technique can be confirmed through multiple methods. For example, molecularly imprinted polymers (MIPs) detect theophylline with high selectivity and stability.

Electrochemical biosensors are used in most biomedical applications. They are popular because they are label-free, low-cost, easy to use, and can be made small. For instance, glucose sensors based on electrochemical detection have made diabetes monitoring cheap and portable. However, the potentiostat is an essential and expensive component in electrochemical biosensing devices. Potentiometric biosensors that employ field-effect transistors for sensing are critical [64]. Imprinting a surface is easy and requires no expensive preparation. Despite some challenges, this old but useful technology has improved [54]. Matrix-assisted laser desorption ionization-time of flight mass spectrometry (MALDI-TOF MS) can confirm the imprint selectivity of the electrochemical surface-imprinting process. Small molecules like peptides can be detected using two-dimensional molecular imprinting. For example, peptide detection shows high specificity using MALDI-TOF MS, proving the method's success.

However, imprinting large molecules is still a problem. Due to their size and molecular weight, proteins are complex to remove from impressions and adhere to surfaces. Using MIPs to create a bio-receptor surface is much cheaper than using antibodies. Detecting biomarkers at low concentrations with ELISA assays is hard. For instance, MIPs designed for the protein bovine serum albumin (BSA) show better durability and reusability than traditional antibody-based systems. These materials are being explored as alternatives to biosensors [84]. Electrode cavities improve sensitivity linearly. Electrochemical biosensors are one of the most essential multiplexed label-free approaches for detecting several analytes [70]. High binding sites and functional groups on protein surfaces can increase non-specific interactions with MIPs, reducing selectivity [85]. Large structures must be made stable by optimizing all parameters and instances. Optimization can employ a similar-sized biomarker protein. MALDI-TOF was a unique approach for testing imprint site specificity, but its sensitivity for big molecular weight proteins remained unknown. In potentiometric detection, factors influence the work function, which changes the golden electrode surface potential when a protein attaches. Surface plasma resonance (SPR) can detect the selectivity of protein binding to imprint cavities.

Exploring the interaction between electrodes and electrolytes, improving surface functionality, and utilizing a three-part setup advance the development of biosensors. These approaches enhance performance, sensitivity, and selectivity, which are essential for a wide range of applications in the diagnostics of biosensors. A multitude of articles utilized a three-electrode system. Every electrode in the system serves a specific function. The working electrode performs the biological process, the reference electrode provides a constant voltage, and the counter electrode provides current. Function separation of electrodes reduces interference and provides accurate measurements [57,86]. To analyze complex electrochemical processes at the electrode-electrolyte interface, the Randles circuit

 doi:10.20944/preprints202503.0996.v1

model is a simple electrical equivalent circuit. It clarifies interface charge transfer, double-layer capacitance, and faradaic reactions. Researchers can extract charge transfer resistance and capacitance, which are crucial for sensor performance, by fitting experimental data into this model. Fitting the Randles circuit model to impedance spectra produces Warburg impedance (W), charge transfer resistance (Rct), solution resistance (Rs), and constant phase element (CPE). Among the four electrical characteristics, Rct is most responsive to electrode changes [62].

$$Z=Rs+Rct+W+1/\ Q(j\omega)n$$

Where:

Z is the total impedance.

Rs is the solution resistance.

Rct is the charge transfer resistance.

W is the Warburg impedance.

Q is the CPE constant.

j represents the imaginary unit.

ω is the angular frequency.

n is the exponent of the CPE.

Electrode functionalization is essential in biosensor construction to successfully immobilize biomolecules. Electrochemical reduction of diazonium cations is the most efficient surface modification method for directing molecules to microarray electrodes [87,88]. This method can regulate the deployment of functional groups on surfaces. Unspecific adsorption on an antibody-functionalized gold surface can be blocked by ethanolamine. It reduces background noise and improves accuracy.

Screen-printed carbon electrodes (SPCE) have the potential for commercialization. The uneven micrometer-level surface of SPCE creates a 3D structure conducive to biomolecular detection [89]. The biosensor exclusively utilizes stainless steel electrodes, resulting in a significant reduction in manufacturing costs [90]. The Randles-Sevcik equation provides insights into the kinetics of electrochemical reactions at electrode surfaces, aiding in the selection of appropriate electrode materials and surface modifications to enhance electron transfer rates and improve biosensor performance. Mathematically, the Randles-Sevcik equation holds significant importance in electrochemistry, particularly in the field of voltammetry. It is represented as:

$$ip = 2.69 * 105\ n^{3/2}\ A\ D^{1/2}\ C\ v^{1/2}$$

where:

- ip represents the peak current (in amperes, A) observed in a voltammetric experiment
- n is the number of electrons transferred in the electrochemical reaction
- A is the electrode area (in square centimeters, cm^2)
- D denotes the diffusion coefficient of the analyte (in square centimeters per second, cm^2/s)
- C represents the concentration of the analyte (in moles per cubic centimeter, mol/cm^3)
- v is the scan rate (in volts per second, V/s)

The Randles-Sevcik equation describes the relationship between peak current and various experimental parameters in cyclic voltammetry. By applying this equation, researchers can analyze and interpret electrochemical data, determine the kinetic parameters of electrochemical reactions, and optimize experimental conditions for voltammetric measurements.

Understanding DNA hybridization enables target identification and peak current, providing a measurable signal indicative of target analyte concentration. Peak current allows for measuring target analytes with high precision and sensitivity by identifying the kinetics of electrochemical processes at the biosensor interface. Developing nucleic acid-detecting electrochemical biosensors requires these concepts. Electrochemical transducers transmit hybridization events into analytical signals effectively. Several literature utilize them to detect DNA hybridization due to their sensitivity, small size, low cost, and microfabrication compliance [91,92]. Detecting hybridization with a redox probe is one method of developing electrochemical DNA biosensors. Due to its distinct interactions with

 doi:10.20944/preprints202503.0996.v1

dsDNA and ssDNA, safranine (SAF) is an excellent hybridization detector [93]. Electrochemical transducers in DNA sensors are effective in immobilizing unmodified oligonucleotides while preserving hybridization. Chemometric methods enhanced electrochemical sensor analysis [94,95]. Electrochemical methods including Chronoamperometry (CA), Linear Sweep Voltammetry (LSV), Potential Step Voltammetry (PSV), and Cyclic Voltammetry (CV) have been extensively utilized to measure and investigate electron transport kinetics on electrode surfaces. For assessing electrolysis and redox processes, these analytical methods are effective [96]. CV and Electrochemical Impedance Spectroscopy (EIS) responses could characterize the alteration phases electrochemically, verifying the method's efficiency. For combined concentration measurement, methods like Square Wave Voltammetry (SWV), PSV, and CA are used together [56]. The highest electron transfer happens at specific voltages unique to each medium, chemistry, and probe-analyte interaction. Peak currents can be used for characteristic correlations using the Cottrell Equation [97] :

$$i = n\,F\,A\,(\pi t)^{-1/2}(\,D\cdot C)^{1/2}$$

where:

i is the current (Amps).

n is the number of electrons transferred in the redox reaction.

F is the Faraday constant (96,485 C/mol).

A is the electrode area (cm^2).

D is the diffusion coefficient (cm^2/s).

C is the concentration of the electroactive species (mol/cm^3).

t is the time (s).

To identify low concentrations of target analytes in complex samples, ECL-RET leverages energy transfer mechanisms to facilitate multiplexed analysis and enhance detection limits. Electrochemical immunosensors based on specific immunological identification are popular due to their simple design, lower detection limit with small sample quantities, rapid process, simplicity of mass manufacturing, and downsizing potential. Electrochemiluminescence resonance energy transfer (ECL-RET) studies trace quantities of diverse targets created by resonance energy transfer between efficient ECL emitters and spectrally matched energy acceptors. The utilization of the ECL-detected model is fundamentally constrained by the initial ECL signal, primarily associated with luminophores' ECL efficiency. ECL resonance energy transfer (ECL-RET) and coreaction are the most effective methods to improve luminophore efficiency [98,99]. Due to the shorter electronic transmission distance and reduced energy loss, intramolecular ECL reaction and ECL-RET increase ECL efficiency and stability compared to standard intermolecular connections [100,101].

In contrast to separate intramolecular coreaction or ECL-RET, the coordinated enhancement merged intramolecular coreaction and RET in the same luminous molecule, increasing ECL efficiency [59]. Analytical models of ECL biosensors include ratiometric and signal-enhanced models, although the quenching-typed biosensor is particularly important for ECL [102,103]. A twofold quenching strategy using one quencher to the same luminous reagent improves quenching-type ECL biosensor sensitivity and ECL technology. Luminol, carbon dots, and other ECL emitters have drawbacks such as reagent waste, limited stability, and the need for additional peroxidase [104]. Luminol immobilization and catalysis can improve the ECL-RET strategy and analytical performance by addressing these problems. Prussian blue analogues (PBAs) are metal-organic frameworks (MOFs) with open three-dimensional structures [105]. Their hollow and porous architectures allow metal cations to be inserted at interstitial sites, creating high biocompatibility, selective adsorption, and electrocatalytic activities. These characteristics imply that PBAs have immense potential as effective catalysts and highly supportive matrices. Since PBAs have poor conductivity and electron transport rates during electrochemistry, they are often combined with noble metallic nanoparticles (NPs), primarily Au NPs [98,99]. More importantly, introducing Ni-Co bimetallic nanozymes to luminol@Au/Ni-Co NCs enhances luminescence efficiency and provides uniform dispersion of Au NPs that form Au–S bonds with DNA strands. Hence, efficient energy acceptors employing ECL-RET

 doi:10.20944/preprints202503.0996.v1

are essential for biosensing analysis. One of the best high-performance ECL energy acceptors is copper sulfide (CuS) [100,101].

3.2. Optical Biosensor

Light-matter interaction is fundamental in optical biosensors as it enables the sensing of biological molecules through changes in light properties. Optimizing optical properties ensures efficient transmission and detection of light within the biosensor. Optical biosensors are accurate but costly. Some of them have photonic crystals. Photonic crystals (PCs) are multilayer structures characterized by periodic changes in the refractive indices of the constituent material layers. The cavity layer thickness, period number, and incidence angle determine the optimal parameters for the compassionate biosensing activity of the structure [106]. The two most critical components of photonic crystals (PCs) are photon localization and the existence of a photonic band gap (PBG). A sharp tunneling peak is generated within the PBG when a particular input light frequency synchronizes with the location of the defect mode. The thickness and refractive index of the defect layer region are substantial determinants of the PBG. Some biosensing photonic devices are based on this fascinating defect mode modulation [107–109].In biosensors that include optical components, the transfer matrix approach aids in comprehending how light interacts with various material layers, coatings, or biological elements on the surface of the sensor. By applying the transfer matrix technique, researchers may estimate and optimize sensor performance by analyzing the effects of variations in material properties, thicknesses, or refractive indices on sensitivity, selectivity, and overall detection capabilities. To examine the influence of salts, proteins, and more minor compounds like vitamins on FRET efficiency in Dulbecco Modified Eagle Medium (DMEM) and a complex artificial wound exudate solution (AWE), FRET efficiency can be evaluated [81]. In optical sensors, FRET is often utilized to translate molecular events or binding events into measurable signals.

Having a large surface area in optical biosensors, such as with porous materials, facilitates higher analyte binding capacity, simultaneously enabling multiple target detection. Biological applications utilize metal nanoclusters because of their unique optical and electrical characteristics [110–114]. Silver nanoclusters (AgNCs), particularly water-soluble DNA-templated AgNCs, have remarkable traits such as facile synthesis, high quantum yield, tunable fluorescence (FL) emission, narrow photoluminescence band, and good biocompatibility [115–117]. AgNCs are ideal for optical materials in biosensing and bioimaging [118,119]. DNA template concentration and reaction time affect AgNC fluorescence. Optimization of sensors should incorporate these parameters. In order to attain substantial enhancements in Raman signals, sample molecules must possess a strong affinity towards the surface of metal nanostructures. Solid substrates give acceptable serum consistency and mild Raman signals [120]. Silver nanoparticles (Ag NPs) were sputtered onto porous silicon/silver composite (PSi/Ag) substrates to form solid substrates. Due to biocompatibility and high surface-to-volume ratios, silicon nanoparticles exhibit excellent homogeneity and reduced toxicity. Washing unreacted bioanalytes from Psi prevents them from interfering with the fluorescent signal. Methods for detecting PSi (porous silicon) fluorescence are more sensitive than those based on the refractive index [121].

Biosensors based on fluorescence detection have a lower limit of detection. A high-resolution spectrophotometer is needed for high-sensitivity detection. The angular spectrum method is used to avoid reflection, but porous silicon shows strong absorption to visible light, which significantly influences the optical properties of porous silicon microcavity (PSM) [122]. Furthermore, visible wavelength laser beams may harm some biological samples. The refractive index change induced by biological reactions in PSM is measured based on the transmission angular spectrum of near-infrared laser light to overcome this issue. The full width at half maximum (FWHM) of the transmitted angle spectrum varies with the Bragg layer cycles, influencing the degree of change in the refractive index produced by transmittance changes. Suppose the Bragg layers are cycled too few times on both sides of the microcavity; the photonic crystal device properties deteriorate. In that case, the FWHM of the

 doi:10.20944/preprints202503.0996.v1

transmitted angular spectrum increases, and detection sensitivity decreases. An excessive number of cycles makes it difficult for biomolecules to incorporate into each layer of the PSM device [76].

Quantum Dots (QDs) are crucial in optical biosensors due to their unique optical properties, including size-tunable emission spectra and high quantum yield.The Stern-Volmer equation is also essential for characterizing the dynamic quenching process in optical biosensors, particularly fluorescence-based assays. QDs are highly photobleach resistant, have narrow and symmetric fluorescence spectra, and exhibit notable fluorescence stability. They are biocompatible and chemically suited to detect biomolecules. QD fluorescence can be enhanced by PSi photonic crystals [123–125]. Attaching a single antibody molecule to multiple QDs reduces the distance between them, which improves dipole interactions among the particles, consequently amplifying Stokes shift and inducing a red shift in the fluorescence spectrum. The reduction in fluorescence intensity could be attributed to protein quenching. Electron transfer may extinguish QD fluorescence when positively charged antibodies combine with negatively charged QDs. Using the PSi Bragg mirror and quantum dots, the biosensor can detect 300 fg/mL by amplifying QD fluorescence [77]. In quenching studies and fluorescence spectroscopy, the Stern-Volmer equation is frequently used. It helps to describe the relationship between the fluorescence intensity of a fluorophore (a molecule that fluoresces) and the concentration of a quencher molecule (a molecule that reduces the fluorescence intensity). The equation estimates quenching reaction efficiency and rate constants. It is helpful for precisely analyzing binding affinities, quenching mechanisms, and molecular interactions [126]. Mathematically, the Stern-Volmer equation is expressed as follows:

$$F0/F = 1 + KSV \cdot [Q]$$

where:

$F0$ is the fluorescence intensity in the absence of a quencher.

F is the fluorescence intensity in the presence of a quencher.

KSV is the Stern-Volmer quenching constant.

$[Q]$ is the concentration of the quencher molecule.

In optical biosensors, PDAN nanoparticles are excellent substrates for immobilizing biomolecules, enhancing sensitivity and stability. PDAN has a non-specific adhesive characteristic, allowing it to adhere to various surfaces. It self-polymerizes to generate coatings that adhere to surfaces like metals, ceramics, polymers, and biological materials. PDAN has numerous promising properties, including solid biocompatibility and extensive UV absorption [127,128]. Primarily, π–π stacking allows for the excellent affinity adsorption of single-stranded DNA on the PDAN surface.

Capillary action plays a crucial role in lateral flow biosensors (LFBs) by facilitating the flow of liquid samples along a porous membrane without the need for external pumps or power sources. The lateral flow biosensor (LFB), one of the most popular testing instruments, is inexpensive, quick to react, easy to use, and compatible [129–133]. LFB has been used in conjunction with nucleic acid-based amplification methods like recombinase polymerase amplification (RPA) and loop-mediated isothermal amplification (LAMP) a lot recently [134–136]. Conversely, these approaches are susceptible to false positive or false negative results caused by nontarget variables such as primer dimers, which are frequently inevitable due to the complexity and unpredictability of genuine clinical samples [137]. CRISPR-associated proteins (Cas) technologies can increase the performance of existing LFBs. Several LFBs have been produced by leveraging trans-collateral activity Cas12a and Cas13a [138–141]. While these approaches have optimal performance, they require extra reactions to conduct the trans-cleavage activity induced by target amplicons, complicating detection. Unlike previous CRISPR systems, CRISPR/Cas9 has excellent recognition ability but no trans-cleavage activity, eliminating time-consuming processes and nontarget factor-induced cleavages [126,142]. Among porous silicon biosensors with various optical architectures, the porous silicon microcavity (PSM) has extremely high sensitivity [143,144]. Porous silicon is utilized in biological diagnostics, veterinary and environmental monitoring, and food quality control.

3.3. Nanomaterial Biosensors

 doi:10.20944/preprints202503.0996.v1

Nanomaterial-based biosensors use carbon dots, nanowires, silver and gold nanoparticles, carbon nanotubes, and graphene quantum dots. They are used in surface modification or as transducers. Despite their benefits, it is essential to consider potential toxicity and validation techniques when using nanomaterials. This section explores the advancements, alternatives, and drawbacks of nanomaterials.

Carbon dots (CDs):

Electrochemical sensing techniques for nanomaterial-modified detection systems have been developed [145–147]. Due to their unique properties, these materials have received much attention. CDs are chemically inert, highly soluble in water, and can be made from various basic materials. They are a promising alternative to quantum dots (QDs) in biolabeling, bioimaging, drug administration, analytical sensing, and photocatalysis. CDs have multiple carboxylic acid groups on their surfaces, making them water soluble and suitable for functionalization with organic, polymeric, inorganic, or biological species. The optical properties of these materials make them excellent fluorescent probes for biological and environmental sensing [148].

Compared to other carbon-based nanomaterials, CDs have not been extensively studied as electrode modifiers for electrochemical biosensors. Research on CDs in electrochemical sensors and biosensors has focused mainly on their electrocatalytic properties for O_2 and H_2O_2 reduction [149–151].

In point-of-care applications, CD-based electrochemical sensors should outperform fluorometric sensors [152]. Additionally, CDs with a significant Stokes shift help differentiate targets from background imaging signals. Carbon nanofibers (CNFs) share the mechanical and electrical characteristics of carbon nanotubes (CNTs) [2.4], but they offer better control over length and diameter. The outer surface of CNFs has more defects than that of CNTs [153]. CNFs provide a high surface area for biomolecule immobilization because they can be functionalized without degrading the carbon backbone structure. CNF-modified electrodes have shown high sensitivity for protein detection [70].

Graphene Quantum Dots:

Graphene quantum dots (GQDs) are innovative materials that can replace expensive and harmful chemical dyes used in laboratories. By adjusting their shape, size, defects, carbon lattice hybridization, functional groups, edge configuration, excitation wavelength, or concentration, it is possible to change their photoluminescence emission from deep ultraviolet to near-infrared [154,155]. Due to edge effects and quantum confinement, GQDs have remarkable electrical and optical properties [156,157]. Bright fluorescence is observed in one study, when GQDs produced at 160°C for 50 minutes [9]. Both bottom-up and top-down techniques can produce GQDs, but the bottom-up technique is better for controlling the shape and size of the product [158].

GQDs can be used to modify electrodes, turning them into nanostructured electrodes with new and exciting features: (1) Carbon nanotube and graphene electrodes have high conductivity in specific directions, accelerating electron transmission [159]. (2) The large surface area of these electrodes helps analyte species adsorb more quickly. (3) Nanostructured materials can be selective and adjustable catalysts, which is helpful for detecting electrocatalysis [160]. (4) The surface chemistry of these systems can be adjusted to manipulate the assembly process for specific capture probes or analyte species [161].

Nanomaterial biosensors effectively detect biomarkers due to their increased surface area for biomolecular interactions. These nanomaterials are often attached to sensor surfaces. The quantum dot–metal ion quenching mechanism includes Forster resonance energy transfer (FRET), the inner filter effect (IFE), and dynamic and static quenching [162]. Graphdiyne (GDY) is highly effective at coating electrode surfaces because of its conductive structure and normal synthesis conditions. Research by Zhu et al. [163] demonstrated that GDY exhibits excellent antibacterial activity and biocompatibility, making it a promising material for biomedical and biosensing applications [163–165].

The NF-kB pathway is significantly stimulated after cells are exposed to various nanoparticles to assess nanoparticle biocompatibility. This pathway is used to evaluate the cytotoxicity of nanoparticles using a cell-based biosensor [166–168]. The sensor cells can detect the harmful effects

 doi:10.20944/preprints202503.0996.v1

of nanoparticles at 10 mg/ml with shorter incubation times. Interestingly, low nanoparticle doses increase cell metabolic activity, suggesting that some nanomaterials can stimulate intracellular repair and defense [169].

Nanowires:

Nanowires are made using special techniques such as lithographic patterning [170]. Recently, scientists have created very long nanowires, sometimes even several millimeters or centimeters long [171]. These nanowires have excellent electrical conductivity and uniform crystal structures and are flexible. However, it is still challenging to align them consistently for practical use. Using ultralong and large-area nanograting templates helps quickly and efficiently create highly ordered nanowire arrays from various materials [172]. For example, wire grid polarizers made with metal nanowires are used in biological applications [173] . Due to their high electrical conductivity, gold nanowires can accelerate electron transport [174].

Silicon nanowire field-effect transistors (SiNW-FETs) are susceptible sensors for proteins [175], cancer markers [137], DNA [176], RNA [177], viruses [178], and other biochemical substances [179–181]. They can detect many biological and chemical species with highly sensitive detection limits lower than the femtomolar limit [179]. They respond to changes in the electric field and other disturbances. In the future, SiNW-FETs could have extremely high sensitivity, direct electrical output, and the ability to detect multiple substances simultaneously [182–184]. Coating silicon nanowires with silicon oxide facilitates the attachment of receptor molecules, allowing for the selective targeting of substances on the SiNW-FET surface [60].

Gold Nanoparticles:

Gold nanoparticles (AuNPs) can detect large molecules and metabolites. Proteins can attach to gold nanoparticles through passive adsorption or covalent bonding [185,186]. Covalent bonding helps avoid several issues with protein attachment. Functional polymers can stabilize gold nanoparticle suspensions by combining them with proteins [187] . Gold nanoprobes are widely used for biosensing, especially for DNA detection [188]. Heterogeneous bimetallic alloy nanoparticles (NPs) have better electrocatalytic activity, charge transfer, and biocompatibility due to their unique properties and interactions [189]. For example, in gold-lead bimetallic alloy NPs (AuPb NPs), the thiol probe coordinates well with both Pb and Au, facilitating attachment to the biosensor surface [190].

Chitosan is commonly used to enhance the production and color of gold nanoparticles. Trifluoromethylsulfonylimide (CS-IL), found in chitosan-1-ethyl-3-methylimidazolium, has low surface tension, promotes nucleation and results in smaller nanoparticles [189]. The interaction between the chitosan amine groups and nanoparticles prevents agglomeration, making CS-IL ideal for creating smaller metallic nanoparticles in larger quantities. Additionally, a covalent bond between the sulfur group of cysteine (Cys) and gold nanoparticles improves the electrochemical response [191,192].

Gold nanoparticles are used as amplifying elements to increase the sensitivity of electrochemical sensors due to their excellent electrocatalytic properties and biocompatibility, especially when placed on a polymer support [193]. Some nanoparticles demonstrate improved catalytic activity due to the combined effect at the metal and polymer support interface, providing more active sites [194].

Silver Nanoparticles:

Silver nanoparticles (AgNps) are commonly used because they are less expensive than gold nanoparticles and have a high interaction energy. They can help to stop the growth of bacteria and fungi and can also help cells grow [195]. Ethanolamine can block unwanted interactions between silver and antibodies, ensuring that only the target molecule interacts with the antibodies. This reduces background noise and improves accuracy [196].

Usually, amines are attached to the surface after hydroxylation, connecting the nanoparticle to the surface. AgNp appears on the electrode if the AgNp is treated with amine and linked to KOH. In the case of electrode modification, KOH can improve the electrical conductivity of the surface [79].

Polymer Dots:

Older biosensors utilized materials such as polydopamine, polyaniline, and graphene. These materials exhibit good electrical conductivity but are not water soluble and are challenging to handle

 doi:10.20944/preprints202503.0996.v1

[197–199]. Polymer dots (PDs) are a better choice. PDs are water soluble, provide good electricity, and are safe for biological use. They have carboxyl (COO-) groups, which help them easily attach to different biomolecules, making biosensors more versatile and sensitive [200–202]. PDs are easy to use in water-based environments and are excellent for biological applications. These features make PDs very useful for creating advanced and effective biosensors [197–199].

Validation Techniques:

Scientists use various methods to determine the structure of nanoparticles. Atomic force microscopy and electron microscopy help visualize the structure. Energy-dispersive X-ray (EDX) analysis confirmed this result. Magnetic nanoparticles are good at separating and enriching target molecules, improving detection sensitivity and specificity [203]. Fourier transform infrared spectroscopy (FTIR) can be used to identify chemical bonds in molecules at specific wavelengths. The zeta potential measures the electrostatic interactions between particles, affecting product performance and nanoparticle stability in a dispersion [63]. UV–Vis absorption and fluorescence spectroscopy were used to analyze the optical properties of the materials, such as DNA–Carbon Dot interactions [204]. Transmission electron microscopy (TEM) images show the nanoparticle size distribution [205]. Fast Fourier transform (FFT) analysis revealed the nanoparticle lattice structure. Raman spectroscopy identifies nanoparticle composition, structure, and interactions by measuring changes in light frequency due to molecular vibrations [63,206].

3.4. Biological Biosensors

This section focuses on valuable materials and efficient techniques for developing biosensors such as whole cells, aptamers, antibody-antigens, and peptide-based biosensors.

1. Whole-cell biosensor

Gram-positive and Gram-negative Bacteria:

Colorimetric and fluorescence-based sensing methods often face problems such as poor reagent stability, low sensitivity, and limited availability of specific antibodies [207–209]. A new method uses antibiotics such as colistin and vancomycin as ligands in bacterial sensors to determine the difference between gram-positive and gram-negative bacteria. This helps doctors quickly prescribe proper treatment [210–213]. Colistin binds to lipopolysaccharide (LPS) in gram-negative bacteria via hydrophobic and ionic interactions [214,215]. Vancomycin forms a hydrogen bond with the D-Ala-D-Ala moiety in the peptidoglycan of gram-positive bacteria [216,217]. By combining colistin and vancomycin with PD, a particular sensor can be created. The sensor can quickly and accurately detect differences between gram-positive and gram-negative bacteria. It can also detect antibiotic-resistant bacteria and can be used for the detection of complex substances such as human serum. Sensors with PD-Colis and PD-Vanco-coated electrodes show exceptional performance in clinical samples, such as human sputum [67].

Secreted alkaline phosphatase (SEAP):

Electrochemical impedance spectroscopy helps study cells on electrodes and analytes in samples, making it useful for real-time monitoring of molecular events [218] . Until recently, there was no biosensor using mammalian cells that was selective for one type of analyte [169].

An impedance biosensor can detect various cell types (such as lung, nasal, skin, and nerve cells). It can identify specific toxins and pathogens related to diseases or environmental toxins [90]. The human-secreted alkaline phosphatase (SEAP) reporter gene, a type of human placental alkaline phosphatase, builds up in a cell culture medium. Its level reflects changes in SEAP gene expression in cells [219]. SEAP, as a secreted reporter protein, has benefits due to its low activity in cell culture medium. This eliminates the need to collect spheroids and allows repeated measurements on the same cultures [220]. Previous studies have used HepG2 cells attached to screen-printed carbon electrodes (SPCEs) for biosensors, although SPCEs are more challenging to make or modify than metal electrodes [221]. A biosensor could be designed in which the SEAP gene product, the enzyme alkaline phosphatase, catalyzes a reaction that produces an electroactive species. This species can

 doi:10.20944/preprints202503.0996.v1

then be detected and quantified using a carbon screen-printed electrode, enabling researchers to monitor the expression of the SEAP gene [222].

3D Cell Culture:

Most whole cell-based biosensors use two-dimensional (2D) cell culture techniques. However, the results from 2D cell cultures often differ from those observed in living animals. This difference is because cells in tissues usually grow in a three-dimensional (3D) environment, unlike the flat culture plates used in laboratories. The reason for this is likely the artificial nature of the culture plate, as most cells in tissues are accustomed to functioning in a three-dimensional environment where many cell connections regulate specialized cell functions.

One significant benefit of 3D cell culture is that it better mimics the extracellular matrix (ECM). The ECM is crucial for cell signaling and function. By incorporating ECM components, 3D cultures provide a more accurate representation of the natural cell environment [169].

Regeneration and Blocking Agents:

Different regeneration agents help reuse electrodes between measurements. These agents must be compatible with the analyte to ensure proper attachment and prevent damage to the sensing surface. According to previous research, BSA-T, 5kPEG, and MCU-T are the most hydrophilic materials used to reduce bacterial attachment to gold electrodes. Among these, BSA-T and MCU-T are the most effective blocking agents [58,223].

2. Antigen-Antibody Biosensors

Ion Concentration Polarization:

Conventional immunoassays are sensitive, fast, efficient, and selective. However, the stability and production cost of antibodies can cause problems, such as inaccurate measurements, complex procedures, and potential environmental harm [53]. Factors such as concentration, temperature, and incubation time are crucial for optimizing antibody assembly [58].

A significant challenge is the movement of antigens from the solution to a nearby antibody by diffusion [56]. Recently, electrical manipulation techniques in microfluidic devices have shown promise for increasing protein concentrations. An ion-selective channel is the best method for creating ion concentration polarization (ICP) in a microfluidic channel. This method traps biomolecules and ions in a tiny volume with good concentrations However, the need for a high-voltage power source (20–80 V) makes it challenging to use in home settings [224].

Biotin:

In biosensors, biotin is often attached to molecules such as antibodies, nucleic acids, or enzymes. These biotinylated molecules are placed on a sensor platform, such as a chip or membrane. Biotin, or vitamin B7, binds strongly to avidin and streptavidin proteins. Streptavidin from Streptomyces avidinii bacteria is used in biotechnology for its strong binding to biotin. This strong noncovalent interaction is widely used in various biochemical assays, diagnostics, and biotechnological applications [53].

Plexiglas:

Plexiglas, known for its clarity and durability, is used to construct a framework or housing for microfluidic channels, detection chambers, or other parts of an immunosensor system. Its transparency allows clear viewing of internal processes, and its durability and ease of production make it ideal for supporting sensor elements [61]. Plexiglas can be molded or laser-cut to create microchannels with precise dimensions, ensuring accurate flow rates and minimal sample volume requirements. This precision is vital for fast and reliable test results, especially in resource-limited settings where the sample volume is limited [225].

3. Peptide Biosensors

Binding affinity:

There are different types of biological biosensors. One crucial type uses antibodies. Electrical biosensors, for instance, use antibodies to detect antigens. When antigens bind to antibodies on the electrode surface, they create a thick, nonconductive coating, increasing the charge transfer resistance (Rct). This thick coating reduces the detection sensitivity [226,227].

 doi:10.20944/preprints202503.0996.v1

Peptide-based biosensors, conversely, do not form bulky layers because peptides are smaller than antibodies. This results in a lower initial Rct and better sensitivity [228,229]. However, peptides have weak affinity and selectivity. An antifouling layer can be added to the sensor to improve this effect, reducing nonspecific adsorption and background noise [230,231].

Improving the binding affinity of peptide probes requires a high density of biorecognition probes on the sensor. Ideally, the probes should be closer together than the size of the target marker [83]. Techniques such as electrografting phenylamine-labeled peptides onto specific layers achieve high probe density, unlike methods such as EDC/NHS coupling, which results in low surface coverage [83].

Using fluorescent and peptide biosensors allows for the selective and sensitive monitoring of specific cell cycle kinases [74,232].

CRISPR/Cas12a:

Combining multiple sensing technologies can overcome individual limitations. For example, integrating hybridization chain reaction (HCR) with CRISPR-Cas12a significantly enhances amplification and detection sensitivity. This allows for identifying even small amounts of biomarkers in serum samples [53].

Using the amplification abilities of the HCR, the CRISPR-Cas12a system has become a versatile sensor for accurately measuring various biomarker products. This method can be adapted for clinical use by utilizing aptamers instead of antibodies to detect biomarkers. Repeating target sequences boosts the CRISPR/Cas12a signal, enhancing sensitivity through HCR amplification and CRISPR-Cas12a trans-cleavage [53].

The approach can also identify multiple receptors simultaneously by controlling dual- or triple-aptamer-based OR logic gate devices in parallel, producing different fluorescence outputs. This approach shows significant promise for standard biomarker detection, facilitating precise clinical diagnoses and effective treatment monitoring [53].

However, performing many processes often leads to unwanted aerosol pollution, which is undesirable for practical use. To fix this, storing all reagents in a lyophilized powder form and incorporating pretreatment, preamplification, CRISPR/Cas9 recognition, and visual analysis into one versatile device can be helpful [71].

Molecular imprinting (MIT):

Molecular recognition is vital for many life systems. Molecular imprinting (MIT) is helpful in creating artificial recognition probes. Protein molecular imprinting polymers (MIPs) have several benefits over antibodies. They are easy and inexpensive to prepare, simple to assemble, have long shelf lives and are stable [233].

However, these devices often face signal interference and low signal-to-noise ratios. This occurs because nonspecific proteins and other components can stick to surfaces through hydrophobic interactions and electrostatic attraction. To address this issue, two key improvements have been made in protein MIP-based biomedical devices. First, antifouling interfaces have been designed to enhance selectivity. Second, protein MIPs with active signal materials have been utilized to improve sensitivity [234–236].

A sensitive and selective protein MIP biosensor was created using conductive and biocompatible GDY and antifouling polyethylene glycol (PEG). This method facilitated the electrochemical detection of the clinical biomarker C-reactive protein (CRP) [1]. Due to the nonconductive PDA film, the GCE coated with the CRP-imprinted PDA film showed a greater EIS signal than did the bare GCE. The antifouling properties of PEG and PDA reduce nonspecific protein adsorption and enhance sensitivity. The molecular imprinting method uses porous, wrinkled, and layered surfaces to remove template protein molecules [1].

Proline:

Proline has a unique cyclic structure with a five-membered ring. Its structure limits its flexibility compared to that of other amino acids. However, the flexibility of proline in molecular recognition and sensing allows it to form versatile molecular structures.

 doi:10.20944/preprints202503.0996.v1

Proline-containing peptides or molecules can fold into different shapes and orientations, providing a dynamic platform for recognizing and interacting with target molecules. The flexibility provided is beneficial for designing recognition elements and enhancing sensitivity and specificity. The specific cyclic structure of proline helps it adopt multiple conformations, making it a flexible recognition element and sensing component [237] .

Chemical Linker:

Substrate cleavage is crucial in biosensor fabrication, especially for enzymatic biosensors. When the target analyte is present, it interacts with the enzyme, starting a reaction that breaks down the substrate into smaller pieces. This process results in a measurable signal. Bovine serum albumin (BSA) or serum can block unwanted binding of enzymes or substrates. High levels of BSA or serum can interfere with substrate cleavage by competing for enzyme binding sites. It reduces the effectiveness of the enzyme. Avoiding chemical linkers can improve biosensors by directly attaching the recognition component to the substrate sequence, increasing the sensitivity of detecting enzyme-induced changes [81].

Isoelectric Point and pH:

The isoelectric point is the pH at which the net charge on the protein is zero. It is important to attach proteins to sensor surfaces. Adjusting the pH can control protein binding or release by changing the surface charge. By enhancing sensor capabilities, the approach captures, detects, or releases specific analytes through protein interactions across various pH levels. Incorrect use of acidic or alkaline solutions near the isoelectric point of the ligand often causes attachment problems. Optimizing conditions before final attachment is necessary to prevent sensor issues, inconsistent data, and wasted electrodes. Preconcentration tests are essential for accurate biomarker detection [54].

pH changes generally affect base signals. Some studies have shown that glycine can regenerate biosensor signals without affecting sensitivity, while others have shown that glycine may permanently change sensor signals. However, using glycine at a pH of 2.0 did not have such effects, with base signal changes remaining below 5% after the fourth cycle [56,238,239].

Self-assembled monolayers (SAMs):

Self-assembled monolayers provide a stable and controlled surface for protein attachment. SAM is versatile and is used in many protein attachment strategies, including the attachment of functional molecules such as SH-ssDNA [240], polyethylene glycol (PEG)-thiol HS-C11-(EG)3-OCH2-COOH [241], the SBP-SPA fusion protein [242,243], and 11-MUA and DTDPA [244]. SAMs can be customized by selecting molecules with different carbon chain lengths and terminal groups, such as COOH or OH, to adjust surface properties and enhance protein stability. For example, molecules such as mercaptohexadecanoic acid (MHDA) with COOH groups or mercaptoundecanol (MUD) with OH groups provide reactive sites for ligand binding while minimizing unwanted interactions [56].

Sensitivity of Biosensors:

Biosensor sensitivity depends greatly on the design and methods used. One study highlighted the importance of these factors [65]. New techniques have been developed to improve sensitivity. One method uses circular electrodes in an electrochemical impedance spectroscopy (EIS) biosensor. The design helps generate electrothermal convection and negative dielectrophoresis (n-DEP). This approach solves issues such as long measurement times and high energy needs in traditional biosensors.

Circular electrodes cause Joule heating. It creates temperature gradients in microfluidic flow regimes [245–247]. These gradients help distribute proteins evenly across the detection area. By using electrokinetic flow and temperature gradients, the biosensor becomes more sensitive. It improves protein capture and detection. This is significant for various bioanalytical uses [65].

Protein Sequencing:

There are several ways to determine the protein sequence in a sample. One method is N-terminal sequencing, also called Edman degradation. This technique involves identifying the amino acid sequence at the N-terminus of a protein or peptide. It is susceptible and can detect minor impurities

 doi:10.20944/preprints202503.0996.v1

or modifications. However, depending on the method used, only the first 10-50 amino acids can be sequenced. It does not provide the entire protein sequence. Another method is sodium dodecyl sulfate–polyacrylamide gel electrophoresis (SDS–PAGE). This technique separates proteins based on their molecular weight. SDS denatures proteins into linear chains, allowing for size-based separation. SDS–PAGE is often a preparatory step for Western blotting, a standard method for detecting specific proteins in a sample [81,248,249].

Surface Modification using Norleucine:

Methionine is often used to modify biosensor surfaces, such as electrodes or nanoparticles. This is because of its hydrophobic sulfur-containing side chain. However, methionine oxidation can negatively affect biomolecule binding and sensor performance. Norleucine, a sulfur-free amino acid analog of methionine, offers a solution to this problem. Biosensors can achieve better stability and reliability by replacing methionine with norleucine in surface modification strategies. The similarity of norleucine to methionine allows it to participate in hydrophobic interactions. It improves molecular binding without the adverse effects of oxidation [250].

4. Nucleic Acid Biosensors

Biofunctionalization:

The time the biosensor spends with single-stranded DNA (ssDNA) is crucial. Optimizing this time is essential. To improve the performance of the biosensor and increase DNA attachment, a mixture of cystine and HAuCl4 can be used to coat gold nanoparticles (AuNPs) onto a gold electrode. The sulfhydryl (–SH) group in cystine is vital for the biological functions of proteins and enzymes. This biofunctionalization process is repeatable, allowing the same number of bioreceptors to bind to the sensor surface, regardless of the DNA sequence or arrangement [80] .

Surface Modification:

The chitosan ionic liquid (CS-IL) layer enhances the performance of the biosensor by increasing its charge transfer resistance (Rct) in the EIS response. This is achieved by forming an insulating layer on the surface of the biosensor. The EIS response is calibrated using the Beer–Lambert Law, relating ssDNA concentration to light absorption. However, there is a need for further improvement in nucleic acid-based biosensing techniques [66]. Due to the unstable nature of sgRNA, a reliable preservation method is necessary.

DNA Walking Machines:

DNA walking machines are artificial molecular machines that have gained attention for their efficiency and ability to handle cargo. Compared with traditional 1D or 2D machines, the new 3D versions offer more advantages. They provide more walking space for complex movements and interactions with target molecules. The improved payload-releasing capabilities of these materials enhance their versatility across numerous applications [59,251].

Recovery rate:

The recovery rate measures how well a system can detect and quantify the target substance in a sample. High recovery rates indicate the ability of the system to accurately measure the desired substance, ensuring reliable analysis results. Low recovery rates may signal losses or interferences that affect accuracy.

To improve recovery rates, analysts can optimize extraction methods, choose appropriate sample preparation techniques, and mitigate matrix effects through sample cleanup procedures. Quality control measures, such as the use of internal standards and calibration curves, help monitor and improve recovery rates. Generally, a recovery rate between 80% and 120% is considered acceptable for many analytical methods [252].

4. Application of Biosensing Techniques

Various biosensors detect rare and dangerous diseases and facilitate early treatment. Biomarkers, measurable indicators of biological processes, disease states, or responses to therapeutic interventions, play a crucial role in developing and validating biosensors. They can be molecules, genes, proteins, or cellular characteristics that indicate normal or pathological biological processes.

 doi:10.20944/preprints202503.0996.v1

Biosensors designed to detect and measure disease-associated biomarkers enable early diagnosis, disease progression monitoring, and treatment efficacy assessment.

4.1. Mesothelioma

Malignant pleural mesothelioma is caused by past asbestos exposure. Asbestos fibers penetrate lung tissue, causing mutations. Mesothelin is a cell surface glycoprotein in normal mesothelial cells [2,253].

Mesothelin can be detected using a quartz crystal microbalance (QCM) biosensor. It can detect approximately 16 mesothelin molecules per Hz, which is equal to 1×10^{-18} g, given that the molecular weight of mesothelin is approximately 40 kDa [69].

Using multiple biomarkers improves cancer detection accuracy. Combining mesothelin, TRX, and fibulin-3 in serum achieved 100% optimized sensitivity and negative predictive value, ensuring detection for further invasive testing for all patients [254].

However, the specificity of serum mesothelin is questionable since its AUC is lower than that of other cancer types and metastases [254]. Plasma fibulin-3 levels (at 52.8 ng/mL) and effusion fibulin-3 levels can effectively differentiate pleural mesothelioma, with a high sensitivity of 96.7% and specificity of 95.5% [255]. No biosensor has been reported to detect this biomarker effectively.

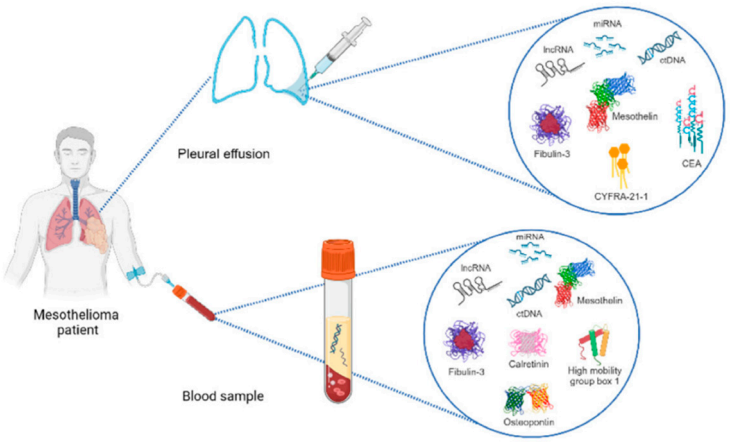

Figure 3. Diagnosing Biomarkers in Pleural Mesothelioma.It shows the workflow for detecting biomarkers to diagnose Pleural Mesothelioma condition [256].

4.2. Hepatoblastoma

Hepatoblastoma (HB) is a malignant tumor that develops from undifferentiated liver progenitor cells and mainly affects children aged six months to three years [8,257]. A 1D defective photonic crystal biosensor can separate primary and secondary tumors, with a sensitivity ranging from 1029.353 to 1240 nm/RIU, depending on the refractive index of the sample [53].Silicon nanowire (SiNW) biosensors are effective for detecting protein biomarkers due to their real-time response, high sensitivity, and label-free detection [60].

Of the five potential genes (ARHGEF2, TMED3, TCF3, STMN1, and RAVER2), only one was significantly upregulated in the HB samples [258]. STMN1, a protein that depolymerizes microtubules, can be used as a diagnostic and therapeutic target for HB. ARHGEF2 has a significant correlation (Cor=0.509, $p<0.05$) with memory B cells, indicating its importance in HB [259,260].

Other studies have confirmed that three proteins, CXCL7, MIF, and IL-25, may be useful for diagnosing and prognosing hepatoblastoma. These factors are strongly linked to clinical stage, lymph node metastasis, vascular invasion, and the serum AFP level but are independent of patient sex, age,

 doi:10.20944/preprints202503.0996.v1

and tumor histological type [261]. Alpha-fetoprotein (AFP) is an essential biological indicator when HB is active and is often used to measure treatment efficacy and patient prognosis [262,263].

Multiplex tumor markers can be identified simultaneously due to the unique optical features of adenine-Ag nanoclusters (A-AgNCs) and cytosine-Ag nanoclusters (C-AgNCs), with AFP and carcinoembryonic antigen (CEA) limits of detection of 2.4 nM and 5.6 nM, respectively [262]. The high fluorescence (FL) quenching ability of polydopamine nanoparticles (PDANs) and the noninterfering FL recovery of AgNCs facilitate the concurrent detection of CEA and AFP, providing an integrated platform for multiplex tumor marker analysis [262]. Although ELISA is rapid, it is ineffective for samples with low AFP concentrations (<100 ng/mL). To address this limitation, an AFP aptamer sensor fused with CRISPR-Cas12a demonstrated a fluorescence intensity proportional to the AFP concentration in the 0.5-104 ng/mL range, with a detection limit of 0.170 ng/mL [53]. Despite various interfering molecules in human serum, the SAT-HCR-CRISPR sensor effectively mitigated interference, enhancing the fluorescence signal for 100 ng/mL AFP more than 10-fold ($p < 0.001$), indicating high selectivity for AFP [53].

4.3. Cystic Echinococcosis

Echinococcosis, a zoonotic disease of global public health concern, is caused by infection of the larval stages of Echinococcus taeniid cestodes [264]. In vitro studies have shown that eosinophilic cationic protein (ECP), a granule protein in eosinophilic granulocytes, exhibits protoscolecidal properties against E. granulosus, with a significant association ($p < 0.05$, $k = 0.56$) with PET-CTI [265]. Traditional methods, such as ELISA and immunoblotting, which detect specific serum antibodies, are labor intensive and time consuming. An electrochemical immunosensor with a detection limit (LOD) of 0.091 ng/mL addresses these limitations by reducing cost and complexity [61]. Additionally, a portable AuNP-based biosensor has been developed to detect low levels of anti-Echinococcus IgG in human and animal blood samples, which is particularly useful in areas lacking controlled infrastructure. The cross-reactivity of the biosensor was evaluated using *Toxoplasma gondii*-positive serum [78].

The low efficiency of Raman spectroscopy (RS) necessitates high laser power and extensive data collection times, potentially damaging biological samples. To overcome this, a rapid and label-free method using surface-enhanced Raman spectroscopy (SERS) has been developed for screening echinococcosis [3]. Hydatid cysts within the abdominal cavity are typically monitored using imaging techniques; however, these techniques are often inconclusive and unsuitable for detecting lung CE or small lesions [266]. High-definition imaging of hydatid cysts is impractical in remote and underdeveloped regions due to the need for sophisticated and costly equipment. Immunological detection methods, while economical, can yield inconsistent results across different detection kits. Antibody detection assays may incorrectly diagnose up to 40% of patients with confirmed CE, and limited detection sensitivity is a challenge for patients with compromised immune responses [267].

Hydatid antigen detection methods are preferred for addressing these issues. A voltammetric immunosensor for detecting hydatid antigens exhibited a detection limit of 0.4 pg/mL and an analytical range of 0.001-100 ng/mL [62]. Additionally, a microcavity biosensor made of porous silicon enables the label-free detection of hydatid disease antigens with a molecular weight of 43 kDa. This biosensor provides a rapid, practical, and cost-effective detection method that is highly suitable for implementation in remote pastoral regions [268].

Furthermore, the detection of the protein kinase P38 has been utilized to diagnose hydatidosis, also known as hydatid disease [269]. As biomarkers for early CE postsurgical outcomes, Eg-cMDH and Eg-CS are promising [266]. To diagnose CE and monitor its potential recurrence following cystectomy, egr-miR-2a-3p levels in the serum may serve as a viable noninvasive biomarker [267]. In one study, in which the area under the curve (AUC) was 0.8176, the level of egr-miR-2a-3p expression was 10.36 times greater before surgery than six months after surgery [62]. By providing healthcare providers with timely information regarding the detection of disease recurrence indicators, these biomarkers enable them to modify treatment strategies accordingly, thereby increasing the likelihood of effective intervention. The prognostic performance of citrate synthase (Eg-CS) and cytoplasmic malate dehydrogenase (Eg-cMDH)

 doi:10.20944/preprints202503.0996.v1

was the highest. Specifically, the probabilities of achieving a "relapse-free" status were 83% and 81%, respectively, if there was a reduction in IgG levels within one month to one year following surgery [78]. This approach facilitates a proactive and focused strategy, which may enhance survival rates and quality of life for those afflicted with recurrent illnesses.

4.4. Cystic Fibrosis

Cystic fibrosis is an autosomal recessive disorder characterized by impaired chloride transport through the epithelial lining of the genitourinary, respiratory, and gastrointestinal tracts, ultimately causing organ injury. CFTR (cystic fibrosis transmembrane conductance regulator) gene mutations cause cystic fibrosis. Prolonged and recurrent respiratory infections, bronchiectasis, and lung failure have the potential to induce substantial morbidity and mortality, whereas spermatic cord obstruction in male patients results in infertility [270] .

Plasma soluble CD14 (sCD14) has been shown to be a potential treatment for CF. With a sensitivity of 82% and a specificity of 100%, plasma sCD14 exhibited a high ROC-AUC value of 0.91 at a cutoff value of 1450 ng/mL [271]. At least 70% of CF patients are reported to have the primary mutation delta F508 in the CFTR gene [272] . In epithelial fluids, CFTR gene mutations increase the chloride ion concentration to 60 mM or greater. A chloride ion concentration less than 20 mM is the critical concentration in these fluids [273]. This reduces chloride reabsorption from perspiration, which produces viscous mucus in various organs [274].

Sweat analysis is a noninvasive alternative to blood analysis, enabling the ongoing monitoring of physiological parameters while minimizing patient discomfort. A chloride ion biosensor utilizing potentiometry is capable of identifying the presence of chloride ions during perspiration at a detection limit of 0.004 mol/m3 [64]. The purpose of the device is to aid in diagnosing cystic fibrosis. Its design considers two adjacent domains: one is an electrolyte containing the desired ions, and the other is a semiconductor [275,276]. As a conventional method for detecting cystic fibrosis (CF), the perspiration chloride test is labor intensive, mandates the expertise of trained personnel, is prone to errors, has a 12% false-negative rate [9], and is laboratory confined. Hence, it is critical to develop portable assays for monitoring circulatory changes (Cl ion detection) to detect cystic fibrosis at the point of care.

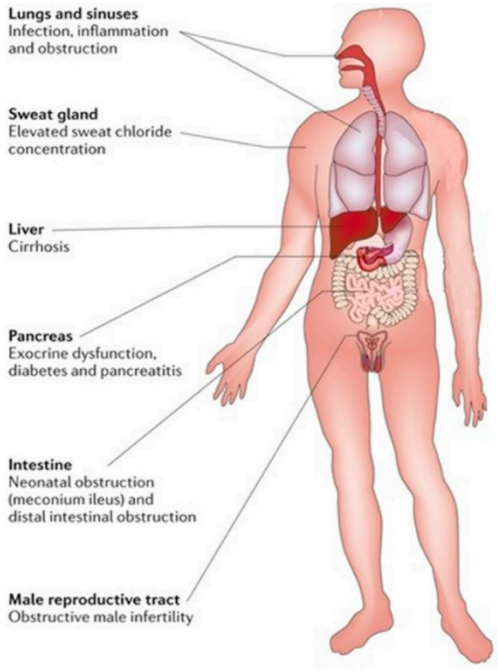

Figure 4. The figure summarizes signs seen in cystic fibrosis patients. It highlights key symptoms across body systems, showing cystic fibrosis's systemic impacts [270].

 doi:10.20944/preprints202503.0996.v1

The quenched fluorescence of graphene quantum dots (GQDs) is a property of the optical sensor utilized in a study to detect chloride ions [271].

Additionally, the ability of GQDs to quench was investigated using potassium chloride as a control to ensure that the observed quenching effect was caused by chloride ions and not cations [9]. Ion exchange chromatography offers high sensitivity and selectivity but is expensive and requires specialized personnel [9]. A label-free detection scheme was implemented, and the voltammetric immunosensor provided a rapid, high-throughput, and cost-effective potential screening method for inherited disorders using only a few droplets of blood [70].

Gene sequencing is the gold standard for identifying these mutations. However, the labor intensiveness and expense of these techniques are significant drawbacks. DNA biosensors offer several benefits, including affordability and ease of use. Unlike conventional DNA sequencing techniques, using electrochemical biosensors to detect specific DNA sequences or mutations can streamline analytical protocols and reduce assay duration. Rapid preventive measures and early diagnosis necessitate implementing these rapid monitoring techniques [277–279]. As an alternative to traditional gene assays, electrochemical DNA biosensors developed using disposable electrodes can be a rapid and accurate screening method for detecting gene mutations [63]. This is achievable without pre modifying the DNA with an alkyl thiol group. The biosensor can detect single nucleotide polymorphisms due to its high selectivity and reproducibility. It has been utilized for the detection of the CFTR gene F508del mutation [63].

Another method for detecting additional proteases, including matrix metalloproteases, cathepsin, and caspases, in multiplex biosensors can potentially be modified by altering the recognition sequence of the peptide biosensor linker. The specificity of this protein-based biosensor, which has been shown to increase up to 500-fold, facilitates the routine surveillance of diseases such as acute respiratory distress syndrome. The compatibility of biosensors with sensing devices, including strips or electrodes, is attributed to their sustained activity when immobilized [81].

4.5. MODY

Patients who exhibit diabetes symptoms before the age of 25 are said to have maturity-onset diabetes of the young (MODY) [5]. Mutations in fourteen genes cause this condition, the most prevalent being GCK-MODY 2 and HNF1A-MODY 3. The disease is often misclassified as TD1 or TD2, leading to a lack of appropriate treatment. Low hs-CRP levels and elevated IL-17A and IL-23 levels serve as potential markers to differentiate MODY3 from other subtypes of MODY [280] .

Although cystatin C is a glomerular filtration rate (GFR) biomarker, it does not affect HNF1A-MODY [281] . Detecting alterations in GCK activity under low glucose conditions presents a challenge. Notably, the FRET distribution was identical for mutation-induced GCK activation, elevated glucose levels, pharmacological GCK activators, and S-nitrosylation. This facilitates the use of a FRET GCK biosensor to monitor GCK enzymatic activity [282]. Despite the availability of laboratory tests for sensors, the challenge lies in detecting readily available biomarkers.

The elution of serum samples using PBS buffer was sufficient to test the electroluminescence sensor design for I27L gene detection [75].Moreover, the sensor provides a versatile framework for identifying additional DNA or RNA molecules [75]. The interlaboratory performance of the N-glycan fucosylation biomarker for HNF1A-MODY was excellent ($r = 0.88$), supporting the development of a diagnostic test that accurately measures antennary fucosylation levels [283]. Clinical utility is indicated by exoglycosidase plate-based assays produced by liquid chromatography and evaluated on 1,000 samples. For the HNF1A MODY biomarker (alpha) 1-3,4 fucosylation, the assay provides favorable outcomes (AUC values of 0.87 and 0.95) [284]. Genetic mutations induce MODY; thus, the biomarkers listed in Table 2 demonstrate high specificity regarding the test region.

 doi:10.20944/preprints202503.0996.v1

Table 2. International Diabetes Analysis.This table analyzes diabetes-related patient information across different countries. It outlines the types of diabetes researched, the markers identified, and clinical metrics to differentiate forms of diabetes. Abbreviation:International Diabetes Analysis.This table analyzes diabetes-related patient information across different countries. It outlines the types of diabetes researched, the markers identified, and clinical metrics to differentiate forms of diabetes. **Abbreviations:** Type 1 Diabetes (T1D), Type 2 Diabetes (T2D), Maturity-Onset Diabetes of the Young (MODY), Glucokinase (GCK), Hepatocyte Nuclear Factor 1-Alpha (HNF1A), Hepatocyte Nuclear Factor 4-Alpha (HNF4A), ATP-Binding Cassette Subfamily C Member 8 (ABCC8), Body Mass Index (BMI), High-Density Lipoprotein (HDL), Connecting Peptide (C-Peptide), High-Sensitivity C-Reactive Protein (hs-CRP), Neonatal Diabetes Mellitus (NDM), Intervening Sequence (IVS).

Country	Patients	Disease	Potential Biomarkers	Reference
China	T1D (n =84); GCK-MODY (n =106); HNF1A-MODY3 (n = 34) ;T2D (n = 82)	T1D, T2D and MODY 2	T1D had higher C-peptide levels and negative antibodies.T2D was characterized by lower body mass index and younger diagnostic age. Further, high-sensitivity C-reactive protein, glycated hemoglobin A1c, 2-h postprandial glucose, and triglyceride were used as indicators for glucokinase-MODY, while triglyceride, high-sensitivity C-reactive protein, and hepatocellular adenoma were used as indicators for hepatocyte nuclear factor 1-a MODY.	[285]
India	HNF1A-MODY3 (n=21), HNF4A-MODY1 (n=10), ABCC8-MODY12 (n=3) , T1D (n=1011) and, T2D (n=1605)	HNF1A-MODY3,HNF4A-MODY1,and ABCC8-MODY12	BMI 21.2–22.7 kg/m2, glycated, hemoglobin 7.2–10%, HDL cholesterol 43–45 mg/dl, fasting C -peptide, 1.2–2.1 ng/ml and stimulated, C-peptide, 2.1–4.5 ng/ml	[286]
Japan	HNF!A_MODY3=1;TD1=41;TD2=65	HNF1A -MODY3	hs-CRP for discriminating MODY3 from type 2 diabetes is 0.5 mg/L,and from type 1 diabetes is 0.26 mg/L	[287]
Italy	TD1=3495;TD2= 37 ;MODY=210;NDM=21 ;Genetic Synddeomes=9 ;Other= 9	GCK and HNF1A	C-peptide level discrimination with TD1 >=0.8 ng/mL	[288]
Russia	n=178	GCK and HNF1A	Mutations in the GCK gene (e.g., p.Lys142*, Leu146Val, Ala173Glnfs30, Val181Asp, Gly261Ala, IVS7 c.864−1G>T, Cys371, Glu443Lys) and in the HNF1A gene (e.g., Ser6Arg, IVS 2 c.526+1 G>T, IVS3 c.713+2 T>A, Arg238Lys) are associated with an increased risk of diabetes, serving as key markers for GCK-MODY and HNF1A-MODY, respectively.	[289]

4.6. Pneumonia

Community-acquired pneumonia (CAP) is characterized by lung infiltration shadows and associated symptoms such as cough, sputum, fever, dyspnea, and chest discomfort on chest radiographs [6]. Previously, pneumonia was primarily diagnosed through smear microscopy, which

 doi:10.20944/preprints202503.0996.v1

is inaccessible in low-income areas. One study utilized an interdigitated microelectrode (IDME) sensing strategy to detect the target "procalcitonin," with an anti-procalcitonin antibody providing a detection limit of 10 ng/mL [79]. However, after the antigen binds to the antibodies on the electrode surface, a sterically massive and nonconductive layer develops, increasing the charge transfer resistance (Rct) and thereby restricting the detection sensitivity [228,229].

Another biosensor detected a significant interaction between the *Streptococcus pneumoniae* analyte and the peptide probe, as evidenced by a dissociation constant of 0.5 nM [83]. Compared to HPLC-UV, a peptide-based biosensor has proven to be affordable, fast, and easy to use, making it a feasible substitute for chromatographic techniques [65]. Electrochemical analyses, known for their portability, label-free nature, high sensitivity, and low cost, present considerable promise in medical diagnosis, including nucleic acids and cells [290–292]. A novel biosensor based on nucleic acids utilizing DNA immobilization and hybridization detected *Legionella pneumophila* with a low limit of quantification (LLOQ) of 1 zeptomolar for severe pneumonia [73].

Procalcitonin and C-reactive protein (CRP) are biomarkers that can differentiate CAP from other lower respiratory tract infections. Hepatic cells produce the 118-kDa pentameric protein known as CRP [293]. The average CRP level in healthy individuals is usually less than 5 mg/L [294]. At a CRP cutoff value of 100 mg/L , the specificity for predicting pneumonia was 91.2% [295]. Using a combined evaluation of CRP and chitinase 3-like-1, a soluble glycoprotein induced by cytokines and harmful stimuli [296], endpoint CAP was distinguished from non endpoint CAP with 80.8% specificity (95% CI 72.6–87.1) and 93% sensitivity (95% CI 76.5–98.8) [297]. The three-host protein test, employing CRP, plasma interferon-γ protein-10 (IP-10), and tumor necrosis factor-related apoptosis-inducing ligand (TRAIL), may provide more significant benefits than previous biomarkers, with 86.7% sensitivity and 91.1% specificity [298].

PCT, a 13 kDa 116 amino acid precursor peptide of calcitonin, was first described in 1975 in scientific publications [299]. Unlike CRP, PCT release is unaffected by systemic steroids [300]. The sensitivity and specificity for separating CAP from COP were 61.1% and 83.9%, respectively, when the PCT threshold value was 0.25 ng/mL [301]. The data gathered from trials where PCT and CRP were compared seem to show that PCT is superior to CRP in determining the etiology of CAP in children; however, the data interpretation may be significantly impacted by the cutoff level used for comparison. According to a study by Moulin et al. [302], PCT demonstrated superior sensitivity, specificity, and positive and negative predictive values to those of CRP with a 60 mg/L threshold.

Nevertheless, the utilization of PCT has its limitations, as values recorded shortly after the onset of symptoms may fall below 0.25 ng/mL [303]. Hence, as directed by PCT-guided algorithms, conducting serial PCT measurements within 6–24 hours is critical. PCT has demonstrated the highest efficacy among conventional biomarkers in bacterial case selection and severity assessment [304]. Another biomarker was sTREM-1, with a sensitivity of 98% and a specificity of 90% when its cutoff value was 5 pg/mL [305]. The utility of sTREM-1 in BAL fluid for the diagnosis of pneumonia was, however, demonstrated by these studies. In general, due to the invasive nature of the procedure, BAL examinations for CAP patients were not performed routinely, particularly in mild to moderate cases.

Table 3. Biosensor Applications in Disease Detection. This table provides a detailed overview of advanced biosensor technologies used to detect various diseases. It highlights detection methods, targeted biomarkers from different sample types, key performance metrics like sensitivity.**Abbreviations:** Malignant Pleural Mesothelioma (MPM), Hyaluronan and Proteoglycan Link Protein 1 (HAPLN1), Tetramethylrhodamine (TAMRA), Cyclin-Dependent Kinase 6 (CDK-6), Interleukin 27 Ligand (I27L), C-Reactive Protein (CRP), Carbon Screen-Printed Electrode (CSPE), Carboxyl Group (COOH), Gold Nanoparticles (AuNPs), Alpha-Fetoprotein (AFP), Carcinoembryonic Antigen (CEA), Phosphate-Buffered Saline (PBS), Cystic Echinococcosis (CE), Alveolar Echinococcosis (AE), Antigen B (AgB), Echinococcus granulosus p38 Antigen (Egp38), Cystic Fibrosis (CF), Fluorescence Resonance Energy Transfer (FRET), Cystic Fibrosis Transmembrane Conductance Regulator (CFTR), Spinal Muscular Atrophy (SMA), Duchenne Muscular Dystrophy (DMD), Survival of Motor Neuron 1 (SMN1), Interdigitated Microelectrode (IDME), Glassy Carbon Electrode (GCE), Ion-Selective Membrane (ISM), Ion-Sensitive Field Effect Transistor (ISFET), Gram-Negative/Gram-Positive (GN/GP), Streptococcus pneumoniae Bacteria (SPB), Mitochondrial Large Subunit Ribosomal RNA (mtLSU rRNA), Poly-Purine Reverse-Hoogsteen (PPRH), Uronic acid Lactonase (UlaG), Legionella pneumophila (L. pneumophila), Macrophage Infectivity Potentiator (mip).

Disease	Biosensor	Bio analyte	Accessibility	Transducer	Bioreceptor	Type of Bioreceptor	Dynamic Range of BS	LOD	Year
MPM	Electrochemical	HAPLN1	Serum	Golden Electrode	Bovine Serum Albumin (BSA)	Amino Acid	-	10^{-9} M	2013 [54]
MPM	Optical	CDK-6	Jurkat Cell Extract	TAMRA Dye	Phosphoamino Acid Binding Domain and 6-phosphofructokinase	Peptide	-	-	2020 [74]
MPM	Gravimetric	Mesothelin	-	Golden Electrode	Mesothelin Antibody	Antibody	100pg/mL- 50 ng/mL	-	2023 [69]
HNF1A-MODY	Optical	I27L gene	-	Bare Glassy Carbon Electrode	Hairpin DNA (S1)	Nucleic Acid	0.0001 - 100 nM	23 fM	2022 [75]
Inflammation; MODY	Electrochemical	CRP	Serum	Electronic Chip with Circularly Arranged Electrodes	Anti-CRP	Antibody	10^{2} - 10^{7} pg/mL	1 pg/mL	2022 [55]
MODY	Electrochemical	CRP	Serum	Carbon Screen Printed Electrodes	Anti-CRP	Antibody	1 - 100 ug/mL	0.058 ug/mL for CSPE-COOH-AuNPs ; 0.085 uG/mL for CSPE-AuNPs-sam	2021 [56]
MODY	Electrochemical	CRP	Blood Sample	Glassy Carbon Electrode	C-reactive protein (CRP) molecularly imprinted polymers (C-MIPs).	Polymer	10^{-5}-10^{3} ng/mL	0.41 × 10^{-5} ng/mL	2021 [1]
MODY	Electrochemical	CRP	Blood Sample	Golden Nanowire	Anti-CRP	Antibody	5 - 220 fg/mL	2.25 fg/mL	2019 [57]
MODY	Electrochemical	C-peptide	Serum	Indium Tin Oxide Electrode	Anti-C-Peptide	Antibody	0.05 ng /mL -100 ng/mL	0.0142 ng/mL	2018 [58]
MODY	Electrochemical	C-peptide	serum	Glassy Carbon Electrode	Anti-C-Peptide	Antibody	50 fg/mL - 16 ng/mL	16.7 fg/mL .	2017 [59]
Hepatoblastoma	Aptamer	AFP	-	Magnetic Beads	AFP Aptamer	Nucleic Acid	0.5 - 10^{4} ng/mL	0.170 ng / mL	2022 [53]
Hepatoblastoma	Optical	AFP; CEA	-	Silver Nanoclusters	AFP and CEA Aptamer	Nucleic Acid	-	AFP is 2.4 nM; CEA is 5.6 nM	2019 [12]
Hepatoblastoma	Optical Microfiber	AFP	-	Single-Mode Optical Fiber	AFP Antibody	Antibody	-	0.2 ng/mL in PBS; 2 ng/mL in bovine serum	2013 [82]
Hepatoblastoma	Electrochemical	AFP	-	Silicon Nanowire	AFP Antibody	Antibody	0.1 - 1 ng/mL	0.1 ng/mL	2015 [60]
Hydatidosis	Electrochemical	Immunoglobulin G Anti-Echinococcus Granulosus Antibodies	Serum	Gold Electrode	E. Granulosus Antigen	Antigen	-	0.091 ng/ ml	2010 [61]

doi:10.20944/preprints202503.0996.v1

Cystic Hydatid	Optical	Cystic Hydatid Antigens	-	Porous Silicon	-	-	0.5 - 20 ng/mL	0.16 ng/ml	2017 [76]
Hydatid Disease	Optical	Egp38 Antigen	-	Porous Silicon	Rabbit Anti-p38	Antibody	0.5 - 15 pg/mL	0.3 pg/mL	2017 [77]
CE; AE	Optical	-	Blood Serum	Porous Silicon with Silver Composite Substrate	-	-	-	-	2019 [3]
CE	Electrochemical	Hydatid Antigen and Antibody	-	Gold Electrode	Rabbit Polyclonal Antibody or Recombinant Antigen B (AgB)	Antigen-Antibody	Antigen:0.001-100 ng/mL; Antibody:0.001-10 ng/mL	Antigen:0.4 pg/mL; Antibody:0.3 pg/mL	2020 [62]
CE	Optical	Anti-Echinococcus Granulosus Antibodies	Blood Sample	Gold Nanoparticles	Hydatid Cyst Antigen	Antigen	-	-	2021 [78]
Hydatid Cyst	Nanoparticle	Anti-E. Granulosus Antibody	Tissue and Serum	Gold Nanoparticles	E. Granulosus Antigen	Antigen	0.001–200 μg/ mL	0.001 μg/ mL	2022 [72]
Inflammation and CF	Optical (FRET)	NE	-	Cyan Fluorescent Protein (CFP) and Yellow Fluorescent Protein (YFP)	Phe-Ile-Arg-Trp (FIRW) sequence	Peptide Linker	-	-	2016 [81]
CF	Electrochemical	373-bases PCR amplicon of exon 11 of CFTR	Blood Smaple	Gold Electrode	CFTR gene	Peptide	-	0.16 nM	2017 [63]
SMA; CF; DMD	Immunosensor	SMN1, CFTR, and DMD proteins	Blood Sample	Carbon Nanofiber	anti-SMN1; anti-CFTR; anti-DMD	Antibody	-	CFTR:0.9 pg/mL, DMD:0.7 pg/mL and SMN1:0.74 pg/mL	2018 [70]
CF	Optical	Cl^-	Sweat Sample	Graphine Quantum Dots (GQD)	ND	ND	10 - 90 mM	10 mM	2022 [9]
CF	Electrochemical	Cl^-	Sweat Sample	Ion-Sensitive Field Effect Transistor (ISFET)	Ion-Selective Membrane (ISM)	Polymer	-	0.004 mol/m^3	2023 [64]
Pneumonia	Immunosensor	Pro-calcitonin	-	Interdigitated Microelectrode (IDME)	Anti-procalcitonin	Antibody	-	10 ng/mL	2023 [71]
Streptococcus pneumoniae	Electrochemical	L-ascorbate 6-phosphate lactonase (AG)	Serum	Glassy Carbon Electrode (GCE)	S7 Peptide	Peptide	-	-	2023 [65]
Mycoplasma Pneumonia	Optical	MP Genome	Sputum Specimen	Golden Nano Particle	ssDNA modified with Thiol (Probe)	Nucleic Acid	3 - 3 × 10^6 copies	3 copies	2023 [79]
Pneumonia	Electrochemical	ssDNA of Pneumococcus	-	Glassy Carbon Electrode (GCE)	Single-stranded DNA modified with Thiol (Probe)	Nucleic Acid	-	impedimetric technique- 3.4 μg/mL; amperometric technique- 21 μg/mL	2022 [66]
Pneumonia	Electrochemical	GN/GP Bacteria	Sputum Specimen	Colistin- and Vancomycin- Electrodes	Colistin- and Vancomycin-Polymer Dot	Polymer	-	gram-negative:3.0 CFU/mL, R^2 :0.995 and gram-positive:3.1 CFU/mL, R^2 :0.994	2022 [67]
Pneumonia, Meningitis	Electrochemical	ss DNA of SPB	-	Glassy Carbon Electrode (GCE)	DNA sequence specific to SPB	Aptamer	-	0.0022 ng/mL	2022 [68]
Pneumocystis Pneumonia	Optical	mtLSU rRNA gene (P. jirovecii)	Lung Fluid	Golden Chip	Poly-Purine Reverse-Hoogsteen PPRH (Probe)	Nucleic Acid	-	2.11 nM	2020 [80]
Streptococcus pneumoniae	Peptide	UlaG	Serum	Carbon Electrode	Aniline-modified S7 Peptide	Peptide	50 - 5 × 10^4 CFU/mL (25% human serum)	-	2019 [83]
Legionnaires (severe pneumonia)	Nucleic Acid	L. pneumophila mip gene	-	Gold Electrode	Probe DNA	Nucleic Acid	1 μM -1 ZM	1 Zepto-molar	2019 [73]

doi:10.20944/preprints202503.0996.v1

 doi:10.20944/preprints202503.0996.v1

6. Conclusion and Future Work

By altering the surface of sensors, it is possible to increase their sensitivity, selectivity, and stability. Electrochemical biosensors are very sensitive and economical and, therefore, suitable for detecting small amounts of nucleic acids. However, the incorporation of nanoparticles can further enhance stability and performance. Additionally, some biomarkers are very precise due to their high sensitivity, even though they are not employed significantly in biosensors. There is a vast scope of biosensor fabrication related to it.

In the case of commercial biosensors, it is crucial to pay attention to aspects such as accuracy, specificity, portability, and stability. Depending on the intended application, selecting the correct type of biosensor is necessary. In the case of emergency rooms, the identification of biomarkers must be performed accurately as soon as possible to make the proper diagnosis. In the case of continuous monitoring, reliability is the most critical factor. Further advancements and new concepts are required to achieve these requirements and incorporate biosensors in clinical and daily practice.

Abbreviation

CFTR	Cystic Fibrosis Transmembrane Conductance Regulator
MODY	Maturity-Onset Diabetes of the Young
3D	Three Dimensional
RBP4	Retinol-binding protein 4
miRNAs	MicroRNAs
LSPR	Localized Surface Plasmon Resonance
MEMS	Micro-Electro-Mechanical Systems
AlN	Aluminum Nitride
COD	Chemical Oxygen Demand
AlGaN	Aluminum Gallium Nitride
GaN	Gallium Nitride
HEMTs	High Electron Mobility Transistors
MOSHEMT	Metal-Oxide-Semiconductor High Electron Mobility Transistor
SAWs	Surface Acoustic Waves
BAWs	Bulk Acoustic Waves

 doi:10.20944/preprints202503.0996.v1

CRISPR–Cas	Clustered Regularly Interspaced Short Palindromic Repeats and CRISPR-associated protein
FET	Field-Effect Transistor
DYRK1A	Dual-specificity Tyrosine-phosphorylation-regulated Kinase 1A
aM	Attomolar
pM	Picomolar
GFET	Graphene Field-Effect Transistor
SiO2	Silicon dioxide
APDMS	3-ethoxy dimethylsilyl propylamine
MMP9	Matrix metalloproteinase 9
CNTs	Carbon nanotubes
PVD	Physical vapor deposition
CVD	Chemical vapor deposition
PA-CVD	Plasma-assisted chemical vapor deposition
HIPIMS	High-power impulse magnetron sputtering
SPCEs	Screen-printed carbon electrodes
CLL	Colloidal Lithography
NiTi	Nickel-Titanium (Nitinol)
CDs	Carbon Dots
QDs	Quantum Dots
O2	Oxygen
H2O2	Hydrogen Peroxide

 doi:10.20944/preprints202503.0996.v1

CNFs	Carbon Nanofibers
GQDs	Graphene Quantum Dots
GDY	Graphdiyne
FRET	Förster Resonance Energy Transfer
IFE	Inner Filter Effect
NF-kB	Nuclear Factor kappa-light-chain-enhancer of activated B cells
SiNW-FETs	Silicon nanowire field-effect transistors
AuNPs	Gold nanoparticles
NPs	Nanoparticles
AuPb NPs	Gold-lead bimetallic alloy nanoparticles
CS-IL	Trifluoromethylsulfonylimide
Cys	Cysteine
AgNPs	Silver nanoparticles
KOH	Potassium Hydroxide
PDs	Polymer Dots
EDX	Energy-dispersive X-ray
FTIR	Fourier Transform Infrared Spectroscopy
TEM	Transmission Electron Microscopy
FFT	Fast Fourier Transform
LPS	Lipopolysaccharide
D-Ala-D-Ala	D-Alanyl-D-Alanine
PD-Colis	Polydopamine-Colistin

 doi:10.20944/preprints202503.0996.v1

PD-Vanco	Polydopamine-Vancomycin
SEAP	Secreted Alkaline Phosphatase
2D	Two-Dimensional
ECM	Extracellular Matrix
BSA-T	Bovine Serum Albumin-Tween
5kPEG	5k Polyethylene Glycol
MCU-T	Mercaptoundecanol-Tween
ICP	Ion Concentration Polarization
Rct	Charge Transfer Resistance
EDC/NHS	N-(3-Dimethylaminopropyl)-N'-ethylcarbodiimide/N-Hydroxysuccinimide
CRISPR/Cas12a	Clustered Regularly Interspaced Short Palindromic Repeats/CRISPR-associated protein 12a
HCR	Hybridization Chain Reaction
CRISPR	Clustered Regularly Interspaced Short Palindromic Repeats
Cas12a	CRISPR-associated protein 12a
CRISPR/Cas9	CRISPR associated protein 9
MIT	Molecular Imprinting Technology
MIPs	Molecular Imprinting Polymers
PEG	Polyethylene Glycol
CRP	C-Reactive Protein
PDA	Polydopamine
EIS	Electrochemical Impedance Spectroscopy

 doi:10.20944/preprints202503.0996.v1

GCE	Glassy Carbon Electrode
BSA	Bovine Serum Albumin
SAM	Self-Assembled Monolayers
SH-ssDNA	Thiol-Modified Single-Stranded DNA
HS-C11-(EG)3-OCH2-COOH	Polyethylene Glycol-Thiol HS-C11-(EG)3-OCH2-COOH
SBP-SPA	Streptavidin-Binding Protein-Streptavidin Protein A
11-MUA	11-Mercaptoundecanoic Acid
DTDPA	Dithiobis [succinimidyl propionate]
MHDA	Mercaptohexadecanoic Acid
MUD	Mercaptoundecanol
n-DEP	Negative Dielectrophoresis
DS–PAGE	Sodium Dodecyl Sulfate–Polyacrylamide Gel Electrophoresis
ssDNA	Single-Stranded DNA
–SH	Sulfhydryl
sgRNA	Single Guide RNA
QCM	Quartz Crystal Microbalance
kDa	kilodaltons
TRX	Thioredoxin
AUC	Area Under the Curve
HB	Hepatoblastoma
SiNW	Silicon Nanowire

 doi:10.20944/preprints202503.0996.v1

ARHGEF2	Rho Guanine Nucleotide Exchange Factor 2
TMED3	Transmembrane Emp24 Protein Transport Domain Containing 3
TCF3	Transcription Factor 3
STMN1	Stathmin 1
RAVER2	Ribonucleoprotein, PTB-Binding 2
RIU	Refractive Index Unit
Cor	Correlation
CXCL7	Chemokine (C-X-C motif) ligand 7
MIF	Macrophage migration inhibitory factor
IL-25	Interleukin-25
AFP	Alpha-fetoprotein
A-AgNCs	Adenine-Ag nanoclusters
C-AgNCs	Cytosine-Ag nanoclusters
CEA	Carcinoembryonic antigen
FL	Fluorescence
PDANs	Polydopamine nanoparticles
ELISA	Enzyme-linked immunosorbent assay
SAT-HCR	Signal Amplification by Templated Hybridization Chain Reaction
ECP	Eosinophilic cationic protein
PET-CTI	Positron Emission Tomography-Computed Tomography Imaging
LOD	Limit of Detection
AuNP	Gold nanoparticles

 doi:10.20944/preprints202503.0996.v1

IgG	Immunoglobulin G
RS	Raman Spectroscopy
SERS	Surface-Enhanced Raman Spectroscopy
CE	Cystic Echinococcosis
Eg-cMDH	Echinococcus granulosus cytoplasmic Malate Dehydrogenase
Eg-CS	Echinococcus granulosus Citrate Synthase
egr-miR-2a-3p	Echinococcus granulosus microRNA-2a-3p
sCD14	soluble CD14
ROC-AUC	Receiver Operating Characteristic - Area Under the Curve
Cl	Chloride
DNA	Deoxyribonucleic Acid
GCK-MODY 2	Glucokinase-Maturity-Onset Diabetes of the Young 2
HNF1A-MODY 3	Hepatocyte Nuclear Factor 1 Alpha-Maturity-Onset Diabetes of the Young 3
TD1	Type 1 Diabetes
TD2	Type 2 Diabetes
hs-CRP	High-sensitivity C-Reactive Protein
IL-17A	Interleukin 17A
IL-23	Interleukin 23
GFR	Glomerular Filtration Rate
HNF1A-MODY	Hepatocyte Nuclear Factor 1 Alpha - Maturity Onset Diabetes of the Young
GCK	Glucokinase
PBS	Phosphate-Buffered Saline

 doi:10.20944/preprints202503.0996.v1

IDME	Interdigitated Microelectrode
HPLC-UV	High-Performance Liquid Chromatography - Ultraviolet
LLOQ	Lower Limit of Quantification
CAP	Community-Acquired Pneumonia
BAL	Bronchoalveolar Lavage

Acknowledgments: The authors would like to express sincere gratitude to the Shreenivas Deshpande Library at the Indian Institute of Technology (BHU) Varanasi for providing invaluable resources and support.

Authors' contributions: DUR: Written original draft; conducted a survey of the literature; prepared the tables; collected the references; methodology; edited and proofread the final manuscript. **GMB:** Guidance on review writing; methodology ; Supervision. All authors have approved the final version of the manuscript.

Funding: No funding was provided for the development of this manuscript.

Availability of data and material: All data relevant to this review are included in the text, references, tables, and figures.

Ethics approval and consent to participate: Not applicable.

Consent for publication: Not applicable.

Competing interests: The authors declare that they have no competing interests.

References

1. Cui, M., et al., A graphdiyne-based protein molecularly imprinted biosensor for highly sensitive human C-reactive protein detection in human serum. Chemical Engineering Journal, 2022. **431**: p. 133455.
2. Opitz, I., et al., ERS/ESTS/EACTS/ESTRO guidelines for the management of malignant pleural mesothelioma. European journal of cardio-thoracic surgery, 2020. **58**(1): p. 1-24.
3. Yue, X., et al., Rapid and label-free screening of echinococcosis serum profiles through surface-enhanced Raman spectroscopy. Analytical and bioanalytical chemistry, 2020. **412**: p. 279-288.
4. Thakur, S., et al., Understanding CFTR Functionality: A Comprehensive Review of Tests and Modulator Therapy in Cystic Fibrosis. Cell Biochemistry and Biophysics, 2024. **82**(1): p. 15-34.
5. Tuerxunyiming, M., et al., Quantitative evaluation of serum proteins uncovers a protein signature related to Maturity-Onset Diabetes of the Young (MODY). Journal of proteome research, 2018. **17**(1): p. 670-679.
6. Mandell, L.A., et al., Infectious Diseases Society of America/American Thoracic Society consensus guidelines on the management of community-acquired pneumonia in adults. Clinical infectious diseases, 2007. **44**(Supplement_2): p. S27-S72.
7. Tomasetti, M., et al., ATG5 as biomarker for early detection of malignant mesothelioma. BMC Research Notes, 2023. **16**(1): p. 61.
8. Schnater, J.M., et al., Where do we stand with hepatoblastoma? Cancer, 2003. **98**(4): p. 668-678.
9. Ifrah, Z., et al., Fluorescence quenching of graphene quantum dots by chloride ions: A potential optical biosensor for cystic fibrosis. Frontiers in Materials, 2022. **9**: p. 857432.

 doi:10.20944/preprints202503.0996.v1

10. Fan, Y., Z. Guo, and G. Ge, Enzyme-Based Biosensors and Their Applications. Biosensors, 2023. **13**(4): p. 476-476.
11. Meskher, H., et al., Recent trends in carbon nanotube (CNT)-based biosensors for the fast and sensitive detection of human viruses: a critical review. Nanoscale advances, 2023. **5**(4): p. 992-1010.
12. Jiang, Y., Y. Tang, and P. Miao, Polydopamine nanosphere@ silver nanoclusters for fluorescence detection of multiplex tumor markers. Nanoscale, 2019. **11**(17): p. 8119-8123.
13. Enrico, A., et al., Cleanroom-Free Direct Laser Micropatterning of Polymers for Organic Electrochemical Transistors in Logic Circuits and Glucose Biosensors. Advanced Science, 2024: p. 2307042.
14. Palmara, G., et al., Functional 3D printing: Approaches and bioapplications. Biosensors and Bioelectronics, 2021. **175**: p. 112849.
15. Fruncillo, S., et al., Lithographic processes for the scalable fabrication of micro-and nanostructures for biochips and biosensors. ACS sensors, 2021. **6**(6): p. 2002-2024.
16. Naresh, V. and N. Lee, A review on biosensors and recent development of nanostructured materials-enabled biosensors. Sensors, 2021. **21**(4): p. 1109.
17. Fan, Y.-F., Z.-B. Guo, and G.-B. Ge, Enzyme-Based Biosensors and Their Applications. Biosensors, 2023. **13**(4): p. 476.
18. Bilge, S., et al., Recent trends in core/shell nanoparticles: their enzyme-based electrochemical biosensor applications. Microchimica Acta, 2024. **191**(5): p. 240.
19. Wang, Q., et al., Research on Fiber Optic Surface Plasmon Resonance Biosensors: A Review. Photonic Sensors, 2024. **14**(2): p. 240201.
20. Lee, M., et al., Recent advances in biological applications of aptamer-based fluorescent biosensors. Molecules, 2023. **28**(21): p. 7327.
21. Sequeira-Antunes, B. and H.A. Ferreira, Nucleic Acid Aptamer-Based Biosensors: A Review. Biomedicines, 2023. **11**(12): p. 3201.
22. Park, J.-H., Y.-S. Eom, and T.-H. Kim, Recent advances in aptamer-based sensors for sensitive detection of neurotransmitters. Biosensors, 2023. **13**(4): p. 413.
23. Léguillier, V., B. Heddi, and J. Vidic, Recent Advances in Aptamer-Based Biosensors for Bacterial Detection. Biosensors, 2024. **14**(5): p. 210.
24. Chen, S., et al., Advances in Synthetic-Biology-Based Whole-Cell Biosensors: Principles, Genetic Modules, and Applications in Food Safety. International Journal of Molecular Sciences, 2023. **24**(9): p. 7989.
25. Hui, C.-y., M.-q. Liu, and Y. Guo, Synthetic bacteria designed using ars operons: a promising solution for arsenic biosensing and bioremediation. World Journal of Microbiology and Biotechnology, 2024. **40**(6): p. 192.
26. Mallozzi, A., et al., A general strategy to engineer high-performance mammalian Whole-Cell Biosensors. bioRxiv, 2024: p. 2024.02. 28.582526.
27. Lo, P.K., Nanometre-Scale Biosensors Revolutionizing Applications in Biomedical and Environmental Research. Biosensors, 2023. **13**(11): p. 969.
28. Balaban Hanoglu, S., et al., Recent Approaches in Magnetic Nanoparticle-Based Biosensors of miRNA Detection. Magnetochemistry, 2023. **9**(1): p. 23.
29. Xia, Q., et al., Advances in Engineered Nano-Biosensors for Bacteria Diagnosis and Multidrug Resistance Inhibition. Biosensors, 2024. **14**(2): p. 59.
30. Ciobanu, D., et al., Recent Progress of Electrochemical Aptasensors toward AFB1 Detection (2018–2023). Biosensors, 2024. **14**(1): p. 7.

 doi:10.20944/preprints202503.0996.v1

31. Singh, A., et al., Recent advances in electrochemical biosensors: Applications, challenges, and future scope. Biosensors, 2021. **11**(9): p. 336.
32. Uniyal, A., et al., Recent advances in optical biosensors for sensing applications: a review. Plasmonics, 2023. **18**(2): p. 735-750.
33. Luo, T., et al., A High-Sensitivity Gravimetric Biosensor Based on S1 Mode Lamb Wave Resonator. Sensors, 2022. **22**(15): p. 5912.
34. Nian, L., et al., Preparation, Characterization, and Application of AlN/ScAlN Composite Thin Films. Micromachines, 2023. **14**(3): p. 557.
35. Gao, F., et al., Acoustic radiation-free surface phononic crystal resonator for in-liquid low-noise gravimetric detection. Microsystems & nanoengineering, 2021. **7**(1): p. 8.
36. Yao, N., J. Wang, and Y. Zhou, Rapid Determination of the Chemical Oxygen Demand of Water Using a Thermal Biosensor. Sensors, 2014. **14**(6): p. 9949-9960.
37. Bouguenna, A., et al., Performance Analysis of AlGaN MOSHEMT Based Biosensors for Detection of Proteins. Transactions on Electrical and Electronic Materials, 2023. **24**(3): p. 188-193.
38. Bhat, A.M., et al., A dielectrically modulated GaN/AlN/AlGaN MOSHEMT with a nanogap embedded cavity for biosensing applications. IETE Journal of Research, 2023. **69**(3): p. 1419-1428.
39. Nair, M.P., A.J.T. Teo, and K.H.H. Li, Acoustic Biosensors and Microfluidic Devices in the Decennium: Principles and Applications. Micromachines, 2022. **13**(1): p. 24.
40. Plikusiene, I. and A. Ramanaviciene, Investigation of biomolecule interactions: Optical-, electrochemical-, and acoustic-based biosensors. Biosensors, 2023. **13**(2): p. 292.
41. Zhang, X., et al., Asymmetric Schottky Barrier-Generated MoS2/WTe2 FET Biosensor Based on a Rectified Signal. Nanomaterials, 2024. **14**(2): p. 226.
42. Hernandez, A.L., et al., Efficient Chemical Surface Modification Protocol on SiO2 Transducers Applied to MMP9 Biosensing. Sensors, 2021. **21**(23): p. 8156.
43. Roh, S., et al., Surface Modification Strategies for Biomedical Applications: Enhancing Cell–Biomaterial Interfaces and Biochip Performances. BioChip Journal, 2023. **17**(2): p. 174-191.
44. Ichou, H., et al., Exploring the advancements in physical vapor deposition coating: a review. Journal of Bio- and Tribo-Corrosion, 2024. **10**(1): p. 3.
45. Khatami, Z., et al., A comprehensive calibration of integrated magnetron sputtering and plasma enhanced chemical vapor deposition for rare-earth doped thin films. Journal of Materials Research, 2024. **39**(1): p. 150-164.
46. Osaki, S., et al., Surface Modification of Screen-Printed Carbon Electrode through Oxygen Plasma to Enhance Biosensor Sensitivity. Biosensors, 2024. **14**(4): p. 165.
47. Abdel-Karim, R., Nanotechnology-enabled biosensors: a review of fundamentals, materials, applications, challenges, and future scope. Biomedical Materials & Devices, 2024. **2**(2): p. 759-777.
48. Minati, L., et al., Plasma assisted surface treatments of biomaterials. Biophysical Chemistry, 2017. **229**: p. 151-164.
49. Topor, C.-V., M. Puiu, and C. Bala, Strategies for Surface Design in Surface Plasmon Resonance (SPR) Sensing. Biosensors, 2023. **13**(4): p. 465.
50. Casalini, S., et al., Self-assembled monolayers in organic electronics. Chemical Society Reviews, 2017. **46**(1): p. 40-71.
51. Sharath Kumar, J., R. Kumar, and R. Verma, Surface Modification Aspects for Improving Biomedical Properties in Implants: A Review. Acta Metallurgica Sinica (English Letters), 2024. **37**(2): p. 213-241.

 doi:10.20944/preprints202503.0996.v1

52. Safavi, M.S., et al., Surface modified NiTi smart biomaterials: Surface engineering and biological compatibility. Current Opinion in Biomedical Engineering, 2023. **25**: p. 100429.
53. Liu, Y., et al., A functionalized magnetic nanoparticle regulated CRISPR-Cas12a sensor for the ultrasensitive detection of alpha-fetoprotein. Analyst, 2022. **147**(14): p. 3186-3192.
54. Mathur, A., et al., Development of a biosensor for detection of pleural mesothelioma cancer biomarker using surface imprinting. PLoS One, 2013. **8**(3): p. e57681.
55. Sheen, H.-J., et al., Electrochemical biosensor with electrokinetics-assisted molecular trapping for enhancing C-reactive protein detection. Biosensors and Bioelectronics, 2022. **210**: p. 114338.
56. Guillem, P., et al., A low-cost electrochemical biosensor platform for C-reactive protein detection. Sensing and Bio-Sensing Research, 2021. **31**: p. 100402.
57. Vilian, A.E., et al., Efficient electron-mediated electrochemical biosensor of gold wire for the rapid detection of C-reactive protein: A predictive strategy for heart failure. Biosensors and Bioelectronics, 2019. **142**: p. 111549.
58. Liu, X., et al., A sensitive electrochemiluminescent biosensor based on AuNP-functionalized ITO for a label-free immunoassay of C-peptide. Bioelectrochemistry, 2018. **123**: p. 211-218.
59. Wang, H., et al., High-sensitive electrochemiluminescence C-peptide biosensor via the double quenching of dopamine to the novel Ru (II)-organic complex with dual intramolecular self-catalysis. Analytical chemistry, 2017. **89**(20): p. 11076-11082.
60. Zhou, F., et al., Highly sensitive, label-free and real-time detection of alpha-fetoprotein using a silicon nanowire biosensor. Scandinavian Journal of Clinical and Laboratory Investigation, 2015. **75**(7): p. 578-584.
61. Pereira, S.V., et al., Microfluidic immunosensor with gold nanoparticle platform for the determination of immunoglobulin G anti-Echinococcus granulosus antibodies. Analytical biochemistry, 2011. **409**(1): p. 98-104.
62. Eissa, S., R. Noordin, and M. Zourob, Voltammetric Label-free Immunosensors for the Diagnosis of Cystic Echinococcosis. Electroanalysis, 2020. **32**(6): p. 1170-1177.
63. García-Mendiola, T., et al., Carbon nanodots based biosensors for gene mutation detection. Sensors and Actuators B: Chemical, 2018. **256**: p. 226-233.
64. la Grasta, A., et al., Potentiometric Chloride Ion Biosensor for Cystic Fibrosis Diagnosis and Management: Modeling and Design. Sensors, 2023. **23**(5): p. 2491.
65. Jalili, F., et al., A novel chemometric-amperometric biosensor for selective and ultra-sensitive determination of Streptococcus pneumoniae based on detection of a protein marker: A suitable and reliable alternative method. Microchemical Journal, 2023. **193**: p. 109122.
66. Yaghoobi, A., et al., An efficiently engineered electrochemical biosensor as a novel and user-friendly electronic device for biosensing of Streptococcus Pneumoniae bacteria. Sensing and Bio-Sensing Research, 2022. **36**: p. 100494.
67. Jo, H.J., et al., Rapid and selective electrochemical sensing of bacterial pneumonia in human sputum based on conductive polymer dot electrodes. Sensors and Actuators B: Chemical, 2022. **368**: p. 132084.
68. Yaghoobi, A., et al., A novel electrochemical biosensor as an efficient electronic device for impedimetric and amperometric quantification of the pneumococcus. Sensing and Bio-Sensing Research, 2022. **37**: p. 100506.
69. Joshi, H.C., et al., Development of a quartz crystal microbalance-based immunosensor for the early detection of mesothelin in cancer. Sensors International, 2023. **4**: p. 100248.

 doi:10.20944/preprints202503.0996.v1

70. Eissa, S., et al., Carbon nanofiber-based multiplexed immunosensor for the detection of survival motor neuron 1, cystic fibrosis transmembrane conductance regulator and Duchenne Muscular Dystrophy proteins. Biosensors and Bioelectronics, 2018. **117**: p. 84-90.
71. Zhu, R., et al., CRISPR/Cas9-based point-of-care lateral flow biosensor with improved performance for rapid and robust detection of Mycoplasma pneumonia. Analytica Chimica Acta, 2023. **1257**: p. 341175.
72. Jafari, F., et al., Design of highly sensitive nano-biosensor for diagnosis of hydatid cyst based on gold nanoparticles. Photodiagnosis and Photodynamic Therapy, 2022. **38**: p. 102786.
73. Mobed, A., et al., An innovative nucleic acid based biosensor toward detection of Legionella pneumophila using DNA immobilization and hybridization: A novel genosensor. Microchemical Journal, 2019. **148**: p. 708-716.
74. Soamalala, J., et al., Fluorescent peptide biosensor for probing CDK6 kinase activity in lung cancer cell extracts. ChemBioChem, 2021. **22**(6): p. 1065-1071.
75. Gong, W., et al., A stochastic DNA walker electrochemiluminescence biosensor based on quenching effect of Pt@ CuS on luminol@ Au/Ni-Co nanocages for ultrasensitive detection of I27L gene. Chemical Engineering Journal, 2022. **434**: p. 134681.
76. Li, P., Z. Jia, and G. Lü, Hydatid detection using the near-infrared transmission angular spectra of porous silicon microcavity biosensors. Scientific Reports, 2017. **7**(1): p. 44798.
77. Li, Y., et al., Detection of Echinococcus granulosus antigen by a quantum dot/porous silicon optical biosensor. Biomedical optics express, 2017. **8**(7): p. 3458-3469.
78. Safarpour, H., et al., Development of optical biosensor using protein a-conjugated chitosan–gold nanoparticles for diagnosis of cystic echinococcosis. Biosensors, 2021. **11**(5): p. 134.
79. Su, L., et al., Synthesised silver nanoparticles mediate interdigitated nanobiosensing for sensitive Pneumonia identification. Materials Express, 2023. **13**(2): p. 246-252.
80. Calvo-Lozano, O., et al., Fast and Accurate Pneumocystis Pneumonia Diagnosis in Human Samples Using a Label-Free Plasmonic Biosensor. Nanomaterials (Basel, Switzerland), 2020. **10**(6): p. E1246-E1246.
81. Schulenburg, C., et al., A FRET-based biosensor for the detection of neutrophil elastase. Analyst, 2016. **141**(5): p. 1645-1648.
82. Li, K., et al., Gold nanoparticle amplified optical microfiber evanescent wave absorption biosensor for cancer biomarker detection in serum. Talanta, 2014. **120**: p. 419-424.
83. Chang, P.-H., et al., An antifouling peptide-based biosensor for determination of Streptococcus pneumonia markers in human serum. Biosensors and Bioelectronics, 2020. **151**: p. 111969.
84. Lavignac, N., C.J. Allender, and K.R. Brain, Current status of molecularly imprinted polymers as alternatives to antibodies in sorbent assays. Analytica chimica acta, 2004. **510**(2): p. 139-145.
85. Jeyachandran, Y.L., et al., Efficiency of blocking of non-specific interaction of different proteins by BSA adsorbed on hydrophobic and hydrophilic surfaces. Journal of colloid and interface science, 2010. **341**(1): p. 136-142.
86. Hasan, M.R., et al., Electrochemical Aptasensor Developed Using Two-Electrode Setup and Three-Electrode Setup: Comprising Their Current Range in Context of Dengue Virus Determination. Biosensors, 2022. **13**(1): p. 1.
87. Randriamahazaka, H. and J. Ghilane, Electrografting and controlled surface functionalization of carbon based surfaces for electroanalysis. Electroanalysis, 2016. **28**(1): p. 13-26.
88. Belanger, D. and J. Pinson, Electrografting: a powerful method for surface modification. Chemical Society Reviews, 2011. **40**(7): p. 3995-4048.

 doi:10.20944/preprints202503.0996.v1

89. Cugnet, C., et al., A novel microelectrode array combining screen-printing and femtosecond laser ablation technologies: Development, characterization and application to cadmium detection. Sensors and Actuators B: Chemical, 2009. **143**(1): p. 158-163.
90. Rozman, M., et al., A HepG2 cell-based biosensor that uses stainless steel electrodes for hepatotoxin detection. Biosensors, 2022. **12**(3): p. 160.
91. Wang, J., Towards genoelectronics: electrochemical biosensing of DNA hybridization. Chemistry–A European Journal, 1999. **5**(6): p. 1681-1685.
92. Paleček, E., Past, present and future of nucleic acids electrochemistry. Talanta, 2002. **56**(5): p. 809-819.
93. Garcia-Mendiola, T., et al., Dyes as bifunctional markers of DNA hybridization on surfaces and mutation detection. Bioelectrochemistry, 2016. **111**: p. 115-122.
94. Esteban, M., C. Arino, and J. Díaz-Cruz, Chemometrics in electroanalytical chemistry. Critical reviews in analytical chemistry, 2006. **36**(3-4): p. 295-313.
95. Grabaric, B., R. O'Halloran, and D. Smith, Resolution enhancement of ac polarographic peaks by deconvolution using the fast fourier transform. Analytica Chimica Acta, 1981. **133**(3): p. 349-358.
96. Dauphin-Ducharme, P., et al., Simulation-based approach to determining electron transfer rates using square-wave voltammetry. Langmuir, 2017. **33**(18): p. 4407-4413.
97. Putzbach, W. and N.J. Ronkainen, Immobilization techniques in the fabrication of nanomaterial-based electrochemical biosensors: A review. Sensors, 2013. **13**(4): p. 4811-4840.
98. Prakash, J., J. Pivin, and H. Swart, Noble metal nanoparticles embedding into polymeric materials: From fundamentals to applications. Advances in colloid and interface science, 2015. **226**: p. 187-202.
99. Sau, T.K., et al., Properties and applications of colloidal nonspherical noble metal nanoparticles. Advanced Materials, 2010. **22**(16): p. 1805-1825.
100. Wang, Y., et al., An energetic CuS–Cu battery system based on CuS nanosheet arrays. ACS nano, 2021. **15**(3): p. 5420-5427.
101. Adhikari, S., D. Sarkar, and G. Madras, Hierarchical design of CuS architectures for visible light photocatalysis of 4-chlorophenol. ACS omega, 2017. **2**(7): p. 4009-4021.
102. Singh, B., et al., Electrochemical transformation of Prussian blue analogues into ultrathin layered double hydroxide nanosheets for water splitting. Chemical Communications, 2020. **56**(95): p. 15036-15039.
103. Zhang, Q., et al., Electrochemical conversion of Fe3O4 magnetic nanoparticles to electroactive Prussian blue analogues for self-sacrificial label biosensing of avian influenza virus H5N1. Analytical chemistry, 2017. **89**(22): p. 12145-12151.
104. Yang, W., et al., PtCo nanocubes/reduced graphene oxide hybrids and hybridization chain reaction-based dual amplified electrochemiluminescence immunosensing of antimyeloperoxidase. Biosensors and Bioelectronics, 2019. **142**: p. 111548.
105. Xu, C., et al., Prussian blue analogues in aqueous batteries and desalination batteries. Nano-micro letters, 2021. **13**: p. 1-36.
106. Malek, C., et al., High Performance Biosensor for Detection of the Normal and Cancerous Liver Tissues Based on 1D Photonic Band Gap Material Structures. Sensing and Imaging, 2023. **24**(1): p. 27.
107. Aly, A.H., et al., MATLAB simulation-based theoretical study for detection of a wide range of pathogens using 1D defective photonic structure. Crystals, 2022. **12**(2): p. 220.
108. Aly, A.H., et al., Study on a one-dimensional defective photonic crystal suitable for organic compound sensing applications. RSC advances, 2021. **11**(52): p. 32973-32980.
109. Aly, A.H., et al., Detection of reproductive hormones in females by using 1D photonic crystal-based simple reconfigurable biosensing design. Crystals, 2021. **11**(12): p. 1533.

 doi:10.20944/preprints202503.0996.v1

110. Nie, S. and S.R. Emory, Probing single molecules and single nanoparticles by surface-enhanced Raman scattering. science, 1997. **275**(5303): p. 1102-1106.
111. Casteleiro, B., et al., Encapsulation of gold nanoclusters by photo-initiated miniemulsion polymerization. Colloids and Surfaces A: Physicochemical and Engineering Aspects, 2022. **648**: p. 129410.
112. Wang, Z., et al., One Stone, Three Birds: Multifunctional Nanodots as "Pilot Light" for Guiding Surgery, Enhanced Radiotherapy, and Brachytherapy of Tumors. ACS Central Science, 2023. **9**(10): p. 1976-1988.
113. Zhang, A., et al., GSH-triggered sequential catalysis for tumor imaging and eradication based on star-like Au/Pt enzyme carrier system. Nano Research, 2020. **13**: p. 160-172.
114. Xie, S., et al., Electrochemical aptasensor based on DNA-templated copper nanoparticles and RecJf exonuclease-assisted target recycling for lipopolysaccharide detection. Analytical Methods, 2024. **16**(3): p. 396-402.
115. Zhou, W. and S. Dong, A new AgNC fluorescence regulation mechanism caused by coiled DNA and its applications in constructing molecular beacons with low background and large signal enhancement. Chemical communications, 2017. **53**(91): p. 12290-12293.
116. Yang, N., et al., Thermal Probing Techniques for a Single Live Cell. Sensors, 2022. **22**(14): p. 5093.
117. Milton, F.P., et al., The chiral nano-world: chiroptically active quantum nanostructures. Nanoscale Horizons, 2016. **1**(1): p. 14-26.
118. Wang, J., et al., Chemical etching of pH-sensitive aggregation-induced emission-active gold nanoclusters for ultra-sensitive detection of cysteine. Nanoscale, 2019. **11**(1): p. 294-300.
119. Zhang, L. and E. Wang, Metal nanoclusters: new fluorescent probes for sensors and bioimaging. Nano Today, 2014. **9**(1): p. 132-157.
120. Jin, H., et al., Research on measurement conditions for obtaining significant, stable, and repeatable SERS signal of human blood serum. IEEE Photonics Journal, 2017. **9**(2): p. 1-10.
121. Krismastuti, F.S., S. Pace, and N.H. Voelcker, Porous silicon resonant microcavity biosensor for matrix metalloproteinase detection. Advanced functional materials, 2014. **24**(23): p. 3639-3650.
122. Li, P., et al., Spectrometer-free biological detection method using porous silicon microcavity devices. Optics Express, 2015. **23**(19): p. 24626-24633.
123. Dorfner, D., et al., Optical characterization of silicon on insulator photonic crystal nanocavities infiltrated with colloidal PbS quantum dots. Applied Physics Letters, 2007. **91**(23).
124. Yang, F. and B.T. Cunningham, Enhanced quantum dot optical down-conversion using asymmetric 2D photonic crystals. Optics Express, 2011. **19**(5): p. 3908-3918.
125. Liu, C., et al., Enhancement of QDs' fluorescence based on porous silicon Bragg mirror. Physica B: Condensed Matter, 2015. **457**: p. 263-268.
126. Yang, W., et al., Detection of CRISPR-dCas9 on DNA with solid-state nanopores. Nano letters, 2018. **18**(10): p. 6469-6474.
127. Wang, C., et al., Skin pigmentation-inspired polydopamine sunscreens. Advanced Functional Materials, 2018. **28**(33): p. 1802127.
128. Wang, Z., et al., High Relaxivity Gadolinium-Polydopamine Nanoparticles. Small, 2017. **13**(43): p. 1701830.
129. Zhang, Q., et al., Optical lateral flow test strip biosensors for pesticides: Recent advances and future trends. TrAC Trends in Analytical Chemistry, 2021. **144**: p. 116427.
130. Sena-Torralba, A., et al., Toward next generation lateral flow assays: Integration of nanomaterials. Chemical Reviews, 2022. **122**(18): p. 14881-14910.
131. Wang, D., et al., Rapid lateral flow immunoassay for the fluorescence detection of SARS-CoV-2 RNA. Nature Biomedical Engineering, 2020. **4**(12): p. 1150-1158.

 doi:10.20944/preprints202503.0996.v1

132. Mao, M., et al., Design and optimizing gold nanoparticle-cDNA nanoprobes for aptamer-based lateral flow assay: Application to rapid detection of acetamiprid. Biosensors and Bioelectronics, 2022. **207**: p. 114114.
133. Yu, S., et al., Development of a lateral flow strip membrane assay for rapid and sensitive detection of the SARS-CoV-2. Analytical Chemistry, 2020. **92**(20): p. 14139-14144.
134. Cherkaoui, D., et al., Harnessing recombinase polymerase amplification for rapid multi-gene detection of SARS-CoV-2 in resource-limited settings. Biosensors and Bioelectronics, 2021. **189**: p. 113328.
135. Ivanov, A.V., et al., Multiplex assay of viruses integrating recombinase polymerase amplification, barcode—anti-barcode pairs, blocking anti-primers, and lateral flow assay. Analytical chemistry, 2021. **93**(40): p. 13641-13650.
136. Li, T., et al., Rapid authentication of mutton products by recombinase polymerase amplification coupled with lateral flow dipsticks. Sensors and Actuators B: Chemical, 2019. **290**: p. 242-248.
137. Zheng, G., et al., Multiplexed electrical detection of cancer markers with nanowire sensor arrays. Nature biotechnology, 2005. **23**(10): p. 1294-1301.
138. Arizti-Sanz, J., et al., Streamlined inactivation, amplification, and Cas13-based detection of SARS-CoV-2. Nature communications, 2020. **11**(1): p. 5921.
139. Broughton, J.P., et al., CRISPR–Cas12-based detection of SARS-CoV-2. Nature biotechnology, 2020. **38**(7): p. 870-874.
140. Zhou, B., et al., CRISPR/Cas12a based fluorescence-enhanced lateral flow biosensor for detection of Staphylococcus aureus. Sensors and Actuators B: Chemical, 2022. **351**: p. 130906.
141. Yue, H., et al., Advances in clustered, regularly interspaced short palindromic repeats (CRISPR)-based diagnostic assays assisted by micro/nanotechnologies. ACS nano, 2021. **15**(5): p. 7848-7859.
142. Hajian, R., et al., Detection of unamplified target genes via CRISPR–Cas9 immobilized on a graphene field-effect transistor. Nature biomedical engineering, 2019. **3**(6): p. 427-437.
143. Zhang, H., et al., Porous silicon optical microcavity biosensor on silicon-on-insulator wafer for sensitive DNA detection. Biosensors and Bioelectronics, 2013. **44**: p. 89-94.
144. Lv, X., et al., Hybridization assay of insect antifreezing protein gene by novel multilayered porous silicon nucleic acid biosensor. Biosensors and Bioelectronics, 2013. **39**(1): p. 329-333.
145. Welch, C.M. and R.G. Compton, The use of nanoparticles in electroanalysis: a review. Analytical and bioanalytical chemistry, 2006. **384**: p. 601-619.
146. Milosavljevic, V., et al., Synthesis of carbon quantum dots for DNA labeling and its electrochemical, fluorescent and electrophoretic characterization. Chemical Papers, 2015. **69**(1): p. 192-201.
147. Katz, E., I. Willner, and J. Wang, Electroanalytical and Bioelectroanalytical Systems Based on Metal and Semiconductor Nanoparticles. Electroanalysis, 2004. **16**(1-2): p. 19-44.
148. Li, H., et al., Carbon nanodots: synthesis, properties and applications. Journal of materials chemistry, 2012. **22**(46): p. 24230-24253.
149. Li, H., et al., Ionic liquid-functionalized fluorescent carbon nanodots and their applications in electrocatalysis, biosensing, and cell imaging. Langmuir, 2014. **30**(49): p. 15016-15021.
150. Ji, H., et al., Nitrogen-doped carbon dots as a new substrate for sensitive glucose determination. Sensors, 2016. **16**(5): p. 630.
151. Wang, Y., et al., Horseradish peroxidase immobilization on carbon nanodots/CoFe layered double hydroxides: direct electrochemistry and hydrogen peroxide sensing. Biosensors and Bioelectronics, 2015. **64**: p. 57-62.

 doi:10.20944/preprints202503.0996.v1

152. Wang, G.-L., et al., Label-free and ratiometric detection of nuclei acids based on graphene quantum dots utilizing cascade amplification by nicking endonuclease and catalytic G-quadruplex DNAzyme. Biosensors and Bioelectronics, 2016. **81**: p. 214-220.
153. Liu, Y.-J., et al., Synthesis of ruthenium (II) complexes and characterization of their cytotoxicity in vitro, apoptosis, DNA-binding and antioxidant activity. European journal of medicinal chemistry, 2010. **45**(7): p. 3087-3095.
154. Lai, S., et al., Mechanisms behind excitation-and concentration-dependent multicolor photoluminescence in graphene quantum dots. Nanoscale, 2020. **12**(2): p. 591-601.
155. Wang, K., et al., Effects of elemental doping on the photoluminescence properties of graphene quantum dots. RSC advances, 2016. **6**(94): p. 91225-91232.
156. Sun, H., et al., Recent advances in graphene quantum dots for sensing. Materials today, 2013. **16**(11): p. 433-442.
157. Lin, L., et al., Luminescent graphene quantum dots as new fluorescent materials for environmental and biological applications. TrAC trends in analytical chemistry, 2014. **54**: p. 83-102.
158. Wu, J., W. Pisula, and K. Müllen, Graphenes as potential material for electronics. Chemical reviews, 2007. **107**(3): p. 718-747.
159. Sanghavi, B.J., et al., Real-time electrochemical monitoring of adenosine triphosphate in the picomolar to micromolar range using graphene-modified electrodes. Analytical chemistry, 2013. **85**(17): p. 8158-8165.
160. Briones, M., et al., Electrocatalytic processes promoted by diamond nanoparticles in enzymatic biosensing devices. Bioelectrochemistry, 2016. **111**: p. 93-99.
161. Swami, N.S., C.-F. Chou, and R. Terbrueggen, Two-potential electrochemical probe for study of DNA immobilization. Langmuir, 2005. **21**(5): p. 1937-1941.
162. Qi, B.-P., et al., An efficient edge-functionalization method to tune the photoluminescence of graphene quantum dots. Nanoscale, 2015. **7**(14): p. 5969-5973.
163. Zhu, Z., et al., Antibacterial activity of graphdiyne and graphdiyne oxide. Small, 2020. **16**(34): p. 2001440.
164. Min, H., et al., Synthesis and imaging of biocompatible graphdiyne quantum dots. ACS applied materials & interfaces, 2019. **11**(36): p. 32798-32807.
165. Jiang, Z., et al., Graphene biosensors for bacterial and viral pathogens. Biosensors and Bioelectronics, 2020. **166**: p. 112471.
166. Prasad, R.Y., et al., Investigating oxidative stress and inflammatory responses elicited by silver nanoparticles using high-throughput reporter genes in HepG2 cells: effect of size, surface coating, and intracellular uptake. Toxicology in vitro, 2013. **27**(6).
167. Stępkowski, T., K. Brzóska, and M. Kruszewski, Silver nanoparticles induced changes in the expression of NF-κB related genes are cell type specific and related to the basal activity of NF-κB. Toxicology in Vitro, 2014. **28**(4): p. 473-478.
168. Chen, J., et al., Inflammatory MAPK and NF-κB signaling pathways differentiated hepatitis potential of two agglomerated titanium dioxide particles. Journal of hazardous materials, 2016. **304**: p. 370-378.
169. Dubiak-Szepietowska, M., et al., A cell-based biosensor for nanomaterials cytotoxicity assessment in three dimensional cell culture. Toxicology, 2016. **370**: p. 60-69.
170. Thurn-Albrecht, T., et al., Ultrahigh-density nanowire arrays grown in self-assembled diblock copolymer templates. Science, 2000. **290**(5499): p. 2126-2129.
171. Xing, Y., et al., Optical properties of the ZnO nanotubes synthesized via vapor phase growth. Applied Physics Letters, 2003. **83**(9): p. 1689-1691.

 doi:10.20944/preprints202503.0996.v1

172. Zubiate, P., et al., High sensitive and selective C-reactive protein detection by means of lossy mode resonance based optical fiber devices. Biosensors and Bioelectronics, 2017. **93**: p. 176-181.
173. Wang, L., et al., High-throughput fabrication of compact and flexible bilayer nanowire grid polarizers for deep-ultraviolet to infrared range. Journal of Vacuum Science & Technology B, 2014. **32**(3): p. 031206.
174. Wang, J., et al., Recent progress in metal nanowires for flexible energy storage devices. Frontiers in Chemistry, 2022. **10**: p. 920430.
175. Zhang, G.-J., et al., An integrated chip for rapid, sensitive, and multiplexed detection of cardiac biomarkers from fingerprick blood. Biosensors and Bioelectronics, 2011. **28**(1): p. 459-463.
176. Gao, A., et al., Silicon-nanowire-based CMOS-compatible field-effect transistor nanosensors for ultrasensitive electrical detection of nucleic acids. Nano letters, 2011. **11**(9): p. 3974-3978.
177. Zhang, G.-J., et al., Label-free direct detection of MiRNAs with silicon nanowire biosensors. Biosensors and Bioelectronics, 2009. **24**(8): p. 2504-2508.
178. Zhang, G.-J., et al., Silicon nanowire biosensor for highly sensitive and rapid detection of Dengue virus. Sensors and Actuators B: Chemical, 2010. **146**(1): p. 138-144.
179. Chen, K.-I., B.-R. Li, and Y.-T. Chen, Silicon nanowire field-effect transistor-based biosensors for biomedical diagnosis and cellular recording investigation. Nano today, 2011. **6**(2): p. 131-154.
180. Lieber, C.M., Semiconductor nanowires: A platform for nanoscience and nanotechnology. Mrs Bulletin, 2011. **36**(12): p. 1052-1063.
181. Chang, K.-S., et al., Monitoring extracellular K+ flux with a valinomycin-coated silicon nanowire field-effect transistor. Biosensors and Bioelectronics, 2012. **31**(1): p. 137-143.
182. Patolsky, F. and C.M. Lieber, Nanowire nanosensors. Materials today, 2005. **8**(4): p. 20-28.
183. Stern, E., et al., Label-free immunodetection with CMOS-compatible semiconducting nanowires. Nature, 2007. **445**(7127): p. 519-522.
184. Bunimovich, Y.L., et al., Quantitative real-time measurements of DNA hybridization with alkylated nonoxidized silicon nanowires in electrolyte solution. Journal of the American Chemical Society, 2006. **128**(50): p. 16323-16331.
185. Geoghegan, W.D. and G.A. Ackerman, Adsorption of horseradish peroxidase, ovomucoid and anti-immunoglobulin to colloidal gold for the indirect detection of concanavalin A, wheat germ agglutinin and goat anti-human immunoglobulin G on cell surfaces at the electron microscopic level: a new method, theory and application. Journal of Histochemistry & Cytochemistry, 1977. **25**(11): p. 1187-1200.
186. Büchel, C., et al., Localisation of the PsbH subunit in photosystem II: a new approach using labelling of His-tags with a Ni2+-NTA gold cluster and single particle analysis. Journal of molecular biology, 2001. **312**(2): p. 371-379.
187. Stobiecka, M. and M. Hepel, Double-shell gold nanoparticle-based DNA-carriers with poly-L-lysine binding surface. Biomaterials, 2011. **32**(12): p. 3312-3321.
188. Veigas, B., et al., One nanoprobe, two pathogens: gold nanoprobes multiplexing for point-of-care. Journal of nanobiotechnology, 2015. **13**: p. 1-7.
189. Safavi, A. and F. Farjami, Electrodeposition of gold–platinum alloy nanoparticles on ionic liquid–chitosan composite film and its application in fabricating an amperometric cholesterol biosensor. Biosensors and Bioelectronics, 2011. **26**(5): p. 2547-2552.
190. Bjørklund, G., et al., A review on coordination properties of thiol-containing chelating agents towards mercury, cadmium, and lead. Molecules, 2019. **24**(18): p. 3247.
191. Zamani-Kalajahi, M., et al., Electrodeposition of taurine on gold surface and electro-oxidation of malondialdehyde. Surface Engineering, 2015. **31**(3): p. 194-201.

 doi:10.20944/preprints202503.0996.v1

192. Jadzinsky, P., et al., Structure of a thiol monolayer-protected gold nanoparticle at 1.1 A resolution. Science (New York, NY), 2007. **318**(5849): p. 430-433.
193. Ming, T., et al., Platinum black/gold nanoparticles/polyaniline modified electrochemical microneedle sensors for continuous in vivo monitoring of pH value. Polymers, 2023. **15**(13): p. 2796.
194. Eisen, C., et al., Hyper crosslinked polymer supported NHC stabilized gold nanoparticles with excellent catalytic performance in flow processes. Nanoscale Advances, 2023. **5**(4): p. 1095-1101.
195. Agnihotri, S., S. Mukherji, and S. Mukherji, Size-controlled silver nanoparticles synthesized over the range 5–100 nm using the same protocol and their antibacterial efficacy. Rsc Advances, 2014. **4**(8): p. 3974-3983.
196. Talib, Z., et al., Frequency Behavior of a Quartz Crystal Microbalance (Qcm) in Contact with Selected Solutions. American Journal of Applied Sciences, 2006. **3**(5): p. 1853-1858.
197. Chen, S., et al., Electrochemiluminescence detection of Escherichia coli O157: H7 based on a novel polydopamine surface imprinted polymer biosensor. ACS applied materials & interfaces, 2017. **9**(6): p. 5430-5436.
198. Chowdhury, A.D., R. Gangopadhyay, and A. De, Highly sensitive electrochemical biosensor for glucose, DNA and protein using gold-polyaniline nanocomposites as a common matrix. Sensors and Actuators B: Chemical, 2014. **190**: p. 348-356.
199. Kurra, N., et al., Laser-derived graphene: A three-dimensional printed graphene electrode and its emerging applications. Nano Today, 2019. **24**: p. 81-102.
200. Kim, S.G., et al., Mitochondria-targeted ROS-and GSH-responsive diselenide-crosslinked polymer dots for programmable paclitaxel release. Journal of Industrial and Engineering Chemistry, 2021. **99**: p. 98-106.
201. Robby, A.I., et al., GSH-responsive self-healable conductive hydrogel of highly sensitive strain-pressure sensor for cancer cell detection. Nano Today, 2021. **39**: p. 101178.
202. Guo, Y., et al., Facilely synthesized pH-responsive fluorescent polymer dots entrapping doped and coupled doxorubicin for nucleus-targeted chemotherapy. Journal of materials chemistry B, 2017. **5**(16): p. 2921-2930.
203. Kosasih, F.U., et al., Nanometric chemical analysis of beam-sensitive materials: a case study of STEM-EDX on perovskite solar cells. Small Methods, 2021. **5**(2): p. 2000835.
204. Wang, C., et al., Magnetic quantum dot based lateral flow assay biosensor for multiplex and sensitive detection of protein toxins in food samples. Biosensors and Bioelectronics, 2019. **146**: p. 111754.
205. Zhang, S. and C. Wang, Precise analysis of nanoparticle size distribution in TEM image. Methods and Protocols, 2023. **6**(4): p. 63.
206. Pilot, R., et al., A review on surface-enhanced Raman scattering. Biosensors, 2019. **9**(2): p. 57.
207. Jiang, G., et al., Fluorescent turn-on sensing of bacterial lipopolysaccharide in artificial urine sample with sensitivity down to nanomolar by tetraphenylethylene based aggregation induced emission molecule. Biosensors and Bioelectronics, 2016. **85**: p. 62-67.
208. Heo, J. and S.Z. Hua, An overview of recent strategies in pathogen sensing. Sensors, 2009. **9**(6): p. 4483-4502.
209. Xiao, L., et al., Colorimetric biosensor for detection of cancer biomarker by Au nanoparticle-decorated Bi2Se3 nanosheets. ACS applied materials & interfaces, 2017. **9**(8): p. 6931-6940.
210. Carrillo-Carrión, C., B.M. Simonet, and M. Valcárcel, Colistin-functionalised CdSe/ZnS quantum dots as fluorescent probe for the rapid detection of Escherichia coli. Biosensors and Bioelectronics, 2011. **26**(11): p. 4368-4374.
211. Shin, C., et al., Rapid naked-eye detection of Gram-positive bacteria by vancomycin-based nano-aggregation. RSC advances, 2018. **8**(44): p. 25094-25103.

 doi:10.20944/preprints202503.0996.v1

212. Qi, G., et al., Vancomycin-modified mesoporous silica nanoparticles for selective recognition and killing of pathogenic gram-positive bacteria over macrophage-like cells. ACS applied materials & interfaces, 2013. **5**(21): p. 10874-10881.
213. Bell, C.S., et al., Magnetic Extraction of Acinetobacter baumannii Using Colistin-Functionalized γ-Fe2O3/Au Core/Shell Composite Nanoclusters. ACS Applied Materials & Interfaces, 2017. **9**(32): p. 26719-26730.
214. Ryu, J.S., et al., Ultra-fast and universal detection of Gram-negative bacteria in complex samples based on colistin derivatives. Biomaterials science, 2020. **8**(8): p. 2111-2119.
215. Khadka, N.K., C.M. Aryal, and J. Pan, Lipopolysaccharide-dependent membrane permeation and lipid clustering caused by cyclic lipopeptide colistin. ACS omega, 2018. **3**(12): p. 17828-17834.
216. Chung, H.J., et al., Ubiquitous detection of gram-positive bacteria with bioorthogonal magnetofluorescent nanoparticles. ACS nano, 2011. **5**(11): p. 8834-8841.
217. Kim, S.J., et al., Structures of Staphylococcus aureus cell-wall complexes with vancomycin, eremomycin, and chloroeremomycin derivatives by 13C {19F} and 15N {19F} rotational-echo double resonance. Biochemistry, 2006. **45**(16): p. 5235-5250.
218. Magar, H.S., R.Y. Hassan, and A. Mulchandani, Electrochemical impedance spectroscopy (EIS): Principles, construction, and biosensing applications. Sensors, 2021. **21**(19): p. 6578.
219. Berger, J., et al., Secreted placental alkaline phosphatase: a powerful new quantitative indicator of gene expression in eukaryotic cells. Gene, 1988. **66**(1): p. 1-10.
220. Dubiak-Szepietowska, M., et al., Development of complex-shaped liver multicellular spheroids as a human-based model for nanoparticle toxicity assessment in vitro. Toxicology and applied pharmacology, 2016. **294**: p. 78-85.
221. Xia, S., et al., Development of a simple and convenient cell-based electrochemical biosensor for evaluating the individual and combined toxicity of DON, ZEN, and AFB1. Biosensors and Bioelectronics, 2017. **97**: p. 345-351.
222. Balbaied, T., A. Hogan, and E. Moore, Electrochemical Detection and Capillary Electrophoresis: Comparative Studies for Alkaline Phosphatase (ALP) Release from Living Cells. Biosensors, 2020. **10**(8): p. 95.
223. Riquelme, M.V., et al., Optimizing blocking of nonspecific bacterial attachment to impedimetric biosensors. Sensing and bio-sensing research, 2016. **8**: p. 47-54.
224. Yoon, J., et al., Simulation and experimental study of ion concentration polarization induced electroconvective vortex and particle movement. Micromachines, 2021. **12**(8): p. 903.
225. Vargas, M.J., et al., Excellent quality microchannels for rapid microdevice prototyping: Direct CO 2 laser writing with efficient chemical postprocessing. Microfluidics and Nanofluidics, 2019. **23**: p. 1-13.
226. Shen, M.-Y., B.-R. Li, and Y.-K. Li, Silicon nanowire field-effect-transistor based biosensors: From sensitive to ultra-sensitive. Biosensors and Bioelectronics, 2014. **60**: p. 101-111.
227. Wei, H., et al., Graphene oxide signal reporter based multifunctional immunosensing platform for amperometric profiling of multiple cytokines in serum. ACS sensors, 2018. **3**(8): p. 1553-1561.
228. Faria, H.A.M. and V. Zucolotto, Label-free electrochemical DNA biosensor for zika virus identification. Biosensors and Bioelectronics, 2019. **131**: p. 149-155.
229. Patil, A.V., et al., Immittance electroanalysis in diagnostics. Analytical chemistry, 2015. **87**(2): p. 944-950.
230. Kuo, T.-M., et al., Facile fabrication of a sensor with a bifunctional interface for logic analysis of the New Delhi metallo-β-lactamase (NDM)-coding gene. ACS Sensors, 2016. **1**(2): p. 124-130.

 doi:10.20944/preprints202503.0996.v1

231. Li, B.-R., et al., Rapid construction of an effective antifouling layer on a Au surface via electrodeposition. Chemical communications, 2014. **50**(51): p. 6793-6796.
232. Peyressatre, M., et al., Identification of quinazolinone analogs targeting CDK5 kinase activity and glioblastoma cell proliferation. Frontiers in Chemistry, 2020. **8**: p. 691.
233. Liu, X., et al., Polydopamine-based molecular imprinted optic microfiber sensor enhanced by template-mediated molecular rearrangement for ultra-sensitive C-reactive protein detection. Chemical Engineering Journal, 2020. **387**: p. 124074.
234. Cui, M., et al., Antifouling sensors based on peptides for biomarker detection. TrAC Trends in Analytical Chemistry, 2020. **127**: p. 115903.
235. Liu, N., et al., Electrochemical aptasensor for ultralow fouling cancer cell quantification in complex biological media based on designed branched peptides. Analytical chemistry, 2019. **91**(13): p. 8334-8340.
236. Cui, M., et al., Mixed self-assembled aptamer and newly designed zwitterionic peptide as antifouling biosensing interface for electrochemical detection of alpha-fetoprotein. ACS sensors, 2017. **2**(4): p. 490-494.
237. Ganguly, H.K. and G. Basu, Conformational landscape of substituted prolines. Biophysical Reviews, 2020. **12**(1): p. 25-39.
238. Goode, J., J. Rushworth, and P. Millner, Biosensor regeneration: a review of common techniques and outcomes. Langmuir, 2015. **31**(23): p. 6267-6276.
239. Xu, M., X. Luo, and J.J. Davis, The label free picomolar detection of insulin in blood serum. Biosensors and Bioelectronics, 2013. **39**(1): p. 21-25.
240. Thangamuthu, M., C. Santschi, and O. JF Martin, Label-free electrochemical immunoassay for C-reactive protein. Biosensors, 2018. **8**(2): p. 34.
241. Bing, X. and G. Wang, Label free C-reactive protein detection based on an electrochemical sensor for clinical application. International Journal of Electrochemical Science, 2017. **12**(7): p. 6304-6314.
242. Kim, C.-H., et al., CRP detection from serum for chip-based point-of-care testing system. Biosensors and Bioelectronics, 2013. **41**: p. 322-327.
243. Lee, H.H., et al., AlGaN/GaN high electron mobility transistor-based biosensor for the detection of C-reactive protein. Sensors, 2015. **15**(8): p. 18416-18426.
244. Fakanya, W.M. and I.E. Tothill, Detection of the inflammation biomarker C-reactive protein in serum samples: towards an optimal biosensor formula. Biosensors, 2014. **4**(4): p. 340-357.
245. Lin, S.-C., et al., A low sample volume particle separation device with electrokinetic pumping based on circular travelling-wave electroosmosis. Lab on a Chip, 2013. **13**(15): p. 3082-3089.
246. Lin, S.-C., et al., An in-situ filtering pump for particle-sample filtration based on low-voltage electrokinetic mechanism. Sensors and Actuators B: Chemical, 2017. **238**: p. 809-816.
247. Lin, S.-C., Y.-C. Tung, and C.-T. Lin, A frequency-control particle separation device based on resultant effects of electroosmosis and dielectrophoresis. Applied Physics Letters, 2016. **109**(5).
248. Petsalaki, E.I., et al., PredSL: a tool for the N-terminal sequence-based prediction of protein subcellular localization. Genomics, Proteomics and Bioinformatics, 2006. **4**(1): p. 48-55.
249. Schägger, H. and G. Von Jagow, Tricine-sodium dodecyl sulfate-polyacrylamide gel electrophoresis for the separation of proteins in the range from 1 to 100 kDa. Analytical biochemistry, 1987. **166**(2): p. 368-379.
250. Pagar, A.D., et al., Recent advances in biocatalysis with chemical modification and expanded amino acid alphabet. Chemical Reviews, 2021. **121**(10): p. 6173-6245.
251. Li, X., et al., A novel ECL biosensor for the detection of concanavalin A based on glucose functionalized NiCo2S4 nanoparticles-grown on carboxylic graphene as quenching probe. Biosensors and Bioelectronics, 2017. **96**: p. 113-120.

 doi:10.20944/preprints202503.0996.v1

252. Williams, M.L., et al., Matrix effects demystified: Strategies for resolving challenges in analytical separations of complex samples. Journal of Separation Science, 2023. **46**(23): p. 2300571.
253. Bayram, M., et al., Serum biomarkers in patients with mesothelioma and pleural plaques and healthy subjects exposed to naturally occurring asbestos. Lung, 2014. **192**: p. 197-203.
254. Sato, H., et al., Droplet digital PCR as a novel system for the detection of microRNA-34b/c methylation in circulating DNA in malignant pleural mesothelioma. International journal of oncology, 2019. **54**(6): p. 2139-2148.
255. Pass, H.I., et al., Fibulin-3 as a blood and effusion biomarker for pleural mesothelioma. New England Journal of Medicine, 2012. **367**(15): p. 1417-1427.
256. Sorino, C., et al., Pleural Mesothelioma: Advances in Blood and Pleural Biomarkers. Journal of Clinical Medicine, 2023. **12**(22): p. 7006.
257. Liu, L., et al., m 6 A mRNA methylation regulates CTNNB1 to promote the proliferation of hepatoblastoma. Molecular Cancer, 2019. **18**: p. 1-13.
258. Liu, S., et al., Construction of a combined random forest and artificial neural network diagnosis model to screening potential biomarker for hepatoblastoma. Pediatric Surgery International, 2022. **38**(12): p. 2023-2034.
259. Bao, P., et al., High STMN1 expression is associated with cancer progression and chemo-resistance in lung squamous cell carcinoma. Annals of Surgical Oncology, 2017. **24**: p. 4017-4024.
260. Yan, L., et al., A novel rapid quantitative method reveals stathmin-1 as a promising marker for esophageal squamous cell carcinoma. Cancer medicine, 2018. **7**(5): p. 1802-1813.
261. Guo, F., et al., Inflammation factors in hepatoblastoma and their clinical significance as diagnostic and prognostic biomarkers. Journal of Pediatric Surgery, 2017. **52**(9): p. 1496-1502.
262. Mussa, A., et al., Defining an optimal time window to screen for hepatoblastoma in children with Beckwith-Wiedemann syndrome. Pediatric blood & cancer, 2019. **66**(1): p. e27492.
263. Feng, J., et al., Assessment of survival of pediatric patients with hepatoblastoma who received chemotherapy following liver transplant or liver resection. JAMA network open, 2019. **2**(10): p. e1912676-e1912676.
264. Becker, H. and L.E. Locascio, Polymer microfluidic devices. Talanta, 2002. **56**(2): p. 267-287.
265. Hotz, J.F., et al., Evaluation of eosinophilic cationic protein as a marker of alveolar and cystic echinococcosis. Pathogens, 2022. **11**(2): p. 261.
266. von Sinner, W.N., New diagnostic signs in hydatid disease; radiography, ultrasound, CT and MRI correlated to pathology. European journal of radiology, 1991. **12**(2): p. 150-159.
267. Craig, P., Detection of specific circulating antigen, immune complexes and antibodies in human hydatidosis from Turkana (Kenya) and Great Britain, by enzyme-immunoassay. Parasite immunology, 1986. **8**(2): p. 171-188.
268. Salah, E.B., et al., Novel biomarkers for the early prediction of pediatric cystic echinococcosis post-surgical outcomes. Journal of Infection, 2022. **84**(1): p. 87-93.
269. Luo, G., et al., Propofol Induces the Expression of Nrf2 and HO-1 in Echinococcus granulosus via the JNK and p38 Pathway In Vitro. Tropical Medicine and Infectious Disease, 2023. **8**(6): p. 306.
270. Meoli, A., et al., State of the Art on Approved Cystic Fibrosis Transmembrane Conductance Regulator (CFTR) Modulators and Triple-Combination Therapy. Pharmaceuticals, 2021. **14**(9): p. 928.
271. Quon, B.S., et al., Plasma sCD14 as a biomarker to predict pulmonary exacerbations in cystic fibrosis. PLoS One, 2014. **9**(2): p. e89341.

 doi:10.20944/preprints202503.0996.v1

272. Cui, K.-H., et al., Optimal polymerase chain reaction amplification for preimplantation diagnosis in cystic fibrosis ((Delta) F508). BMJ, 1995. **311**(7004): p. 536-540.
273. Quinton, P.M., Chloride impermeability in cystic fibrosis. Nature, 1983. **301**(5899): p. 421-422.
274. Esteves, C.Z., et al., Skin biomarkers for cystic fibrosis: A potential non-invasive approach for patient screening. Frontiers in pediatrics, 2018. **5**: p. 290.
275. Farrell, P.M., et al., Early diagnosis of cystic fibrosis through neonatal screening prevents severe malnutrition and improves long-term growth. Pediatrics, 2001. **107**(1): p. 1-13.
276. LeGrys, V.A., et al., Diagnostic sweat testing: the Cystic Fibrosis Foundation guidelines. The Journal of pediatrics, 2007. **151**(1): p. 85-89.
277. Miao, P., et al., An electrochemical sensing strategy for ultrasensitive detection of glutathione by using two gold electrodes and two complementary oligonucleotides. Biosensors and Bioelectronics, 2009. **24**(11): p. 3347-3351.
278. Wang, J., Electrochemical biosensors: towards point-of-care cancer diagnostics. Biosensors and Bioelectronics, 2006. **21**(10): p. 1887-1892.
279. Paleček, E., et al., Electrochemical biosensors for DNA hybridization and DNA damage. Biosensors and Bioelectronics, 1998. **13**(6): p. 621-628.
280. Diren, A., et al., Cytokine Profile in Patients With Maturity onset Diabetes of the Young. In Vivo, 2022. **36**(5): p. 2490-2504.
281. Acaralp, S. and H. Akhondi, Systematic Survey of Creatinine-Based Versus Cystatin C-based Estimated GFR in People with Diabetes. HCA Healthcare Journal of Medicine, 2020. **1**(4): p. 231-246.
282. Seckinger, K.M., et al., Nitric oxide activates β-cell glucokinase by promoting formation of the "glucose-activated" state. Biochemistry, 2018. **57**(34): p. 5136-5144.
283. Demus, D., et al., Interlaboratory evaluation of plasma N-glycan antennary fucosylation as a clinical biomarker for HNF1A-MODY using liquid chromatography methods. Glycoconjugate journal, 2021. **38**: p. 375-386.
284. Demus, D., et al., Development of an exoglycosidase plate-based assay for detecting α1-3, 4 fucosylation biomarker in individuals with HNF1A-MODY. Glycobiology, 2022. **32**(3): p. 230-238.
285. Fu, J., et al., A clinical prediction model to distinguish maturity-onset diabetes of the young from type 1 and type 2 diabetes in the Chinese population. Endocrine Practice, 2021. **27**(8): p. 776-782.
286. Aarthy, R., et al., Identification of appropriate biochemical parameters and cut points to detect Maturity Onset Diabetes of Young (MODY) in Asian Indians in a clinic setting. Scientific Reports, 2023. **13**(1): p. 11408.
287. Ohki, T., et al., Low serum level of high-sensitivity C-reactive protein in a J apanese patient with maturity-onset diabetes of the young type 3 (MODY3). Journal of diabetes investigation, 2014. **5**(5): p. 513-516.
288. Delvecchio, M., et al., Monogenic diabetes accounts for 6.3% of cases referred to 15 Italian pediatric diabetes centers during 2007 to 2012. The Journal of Clinical Endocrinology & Metabolism, 2017. **102**(6): p. 1826-1834.
289. Ivanoshchuk, D.E., et al., The mutation spectrum of maturity onset diabetes of the young (MODY)-associated genes among Western Siberia patients. Journal of personalized medicine, 2021. **11**(1): p. 57.
290. Huang, S.-H., et al., Detection of serum uric acid using the optical polymeric enzyme biochip system. Biosensors and Bioelectronics, 2004. **19**(12): p. 1627-1633.
291. Li, B.-R., et al., An ultrasensitive nanowire-transistor biosensor for detecting dopamine release from living PC12 cells under hypoxic stimulation. Journal of the American Chemical Society, 2013. **135**(43): p. 16034-16037.

 doi:10.20944/preprints202503.0996.v1

292. Zhang, G.-J. and Y. Ning, Silicon nanowire biosensor and its applications in disease diagnostics: a review. Analytica chimica acta, 2012. **749**: p. 1-15.
293. Mortensen, R.F., C-reactive protein, inflammation, and innate immunity. Immunologic research, 2001. **24**: p. 163-176.
294. Du Clos, T.W., C-reactive protein as a regulator of autoimmunity and inflammation. Arthritis & Rheumatism, 2003. **48**(6): p. 1475-1477.
295. Gencay, M., Diagnostic value of signs, symptoms and laboratory values in lower respiratory tract infection. Swiss Medical Weekly, 2006. **136**(2728): p. 434-434.
296. Coffman, F.D., Chitinase 3-Like-1 (CHI3L1): a putative disease marker at the interface of proteomics and glycomics. Critical reviews in clinical laboratory sciences, 2008. **45**(6): p. 531-562.
297. Erdman, L.K., et al., Biomarkers of host response predict primary end-point radiological pneumonia in Tanzanian children with clinical pneumonia: a prospective cohort study. PloS one, 2015. **10**(9): p. e0137592.
298. van Houten, C.B., et al., A host-protein based assay to differentiate between bacterial and viral infections in preschool children (OPPORTUNITY): a double-blind, multicentre, validation study. The Lancet Infectious Diseases, 2017. **17**(4): p. 431-440.
299. Moya, F., A. Nieto, and J.L. R-CANDELA, Calcitonin biosynthesis: evidence for a precursor. European journal of biochemistry, 1975. **55**(2): p. 407-413.
300. Annane, D., Prohormones: novel biomarkers for corticosteroids in septic shock? Intensive care medicine, 2008. **34**(3): p. 395-396.
301. Ito, A., et al., Utility of procalcitonin for differentiating cryptogenic organising pneumonia from community-acquired pneumonia. Clinical Chemistry and Laboratory Medicine (CCLM), 2019. **57**(10): p. 1632-1637.
302. Moulin, F., et al., Procalcitonin in children admitted to hospital with community acquired pneumonia. Archives of disease in childhood, 2001. **84**(4): p. 332-336.
303. Schuetz, P., W. Albrich, and B. Mueller, Procalcitonin for diagnosis of infection and guide to antibiotic decisions: past, present and future. BMC medicine, 2011. **9**: p. 1-9.
304. Principi, N. and S. Esposito, Biomarkers in pediatric community-acquired pneumonia. International journal of molecular sciences, 2017. **18**(2): p. 447.
305. Gibot, S., et al., Soluble triggering receptor expressed on myeloid cells and the diagnosis of pneumonia. New England Journal of Medicine, 2004. **350**(5): p. 451-458.